

DEVELOPMENT OF MULTIFUNCTIONAL
NANOFIBROUS MEMBRANE MATERIAL FOR
BIOLOGICAL WASTEWATER TREATMENT

ESRAT JAHAN

A THESIS SUBMITTED TO
THE FACULTY OF GRADUATE STUDIES
IN PARTIAL FULFILLMENT OF THE REQUIREMENTS
FOR THE DEGREE OF
MASTER OF APPLIED SCIENCE

GRADUATE PROGRAM IN MECHANICAL ENGINEERING
YORK UNIVERSITY
TORONTO, ONTARIO

July 2021

© Esrat Jahan, 2021

Abstract

In this study, a hybrid multifunctional membrane, which integrates a polymer-based electrospun nanofibrous membrane to a macro-porous open-foam biofilm carrier, is developed and fabricated for membrane bioreactor applications. In particular, the membrane will have to satisfy two functional requirements: (i) improving filtration performance by alleviating membrane fouling; and (ii) enhancing sustainable growth of biofilm for improved organic removal. The nanofibrous membrane, consisting of polyvinylidene fluoride (PVDF) and multiwalled carbon nanotube (MWCNT) was prepared by electrospinning. The open-cell biofilm carrier was fabricated by compression molding and salt leaching using PVDF. Then, the adhesion of the nanofibrous membrane to the open-cell foam was achieved at elevated temperature with the assistance by supercritical carbon dioxide (ScCO₂).

The effects of processing parameters of the electrospinning process and material formulation on the morphology of the membrane have been investigated and then the effect of MWCNT loading on the filtration performance of the membranes were investigated.

Acknowledgement

I would like to express the deepest gratitude to my research supervisors, Professor. Leung and Professor. Eldyasti for their encouragement, guidance, support during the period of my research work.

I would also like to express my gratitude to my friends, colleagues, and family to provide me the emotional support during the period of my master's studies.

Table of Contents

Abstract	ii
Acknowledgement	iii
Table of Contents	iv
List of Tables	vii
List of Figures	viii
List of Abbreviations.....	xi
Chapter One: Preamble	1
1.1. Introduction	1
1.2 Research Motivation	3
1.3. Research Objectives.....	4
1.4. Thesis structure.....	5
Chapter Two: Background and Literature Review	6
2.1. Biological Wastewater Treatment	6
2.2 Membrane Applications in Biological Wastewater Treatment	8
2.3. Membrane fabrication methods	10
2.3.2. Interfacial polymerization.....	11
2.3.3 Stretching.....	12
2.3.4. Track etching.....	13
2.3.5 Electrospinning	13
2.4. Foam	14
2.4.1 Open-cell foam fabrication methods	15
2.4.1.1 Thermally induced phase separation	15
2.4.1.2. Emulsion freeze drying.....	16
2.4.1.3. Particulate leaching	16
2.5. Effect of processing parameter on electrospinning	16
2.5.1. Applied Voltage	17
2.5.2 Flow rate of polymer solution.....	18
2.5.3. Tip-to-collector separation distance	19
2.6. Fouling in membranes.....	19
2.6.1. Classification of foulants	21
2.6.1.1 Biofoulants	21

2.6.1.2. Organic foulants.....	22
2.6.1.3. Inorganic fouling.....	23
2.7. Factors effecting membrane fouling	24
2.7.1. Membrane material.....	24
2.7.1.1. Polyvinylidene fluoride membranes	25
2.7.1.2. Polyethersulfone in membranes.....	27
2.7.1.3. Polysulfone in membranes	28
2.7.1.4. Polyacrylonitrile in membranes	29
2.7.2. Hydrophilicity and hydrophobicity of membranes	30
2.7.3. Membrane surface charge.....	31
2.7.4. Membrane surface roughness	31
2.8 Technology gap	32
Chapter Three: Effect of processing parameter of electrospinning on nanofibrous membrane	33
3.1 Experimental	33
3.1.1 Materials	33
3.1.2. Preparation of electrospun membrane	33
3.1.3. Characterization	34
3.2. Results and discussion	36
3.2.1. Effect of flow rate on the morphology	36
3.2.2. Effect of applied voltage on the morphology	37
3.2.3. Effect of tip-to-collector distance on the morphology	39
3.2.4 Effect of MWCNT contents on the morphology	40
3.3 Conclusion.....	41
Chapter Four: Multifunctional membrane system in wastewater treatment	43
4.1 Experimental	44
4.1.1. Materials	44
4.1.2. Preparation of open-cell foam.....	44
4.1.4. Preparation of multifunctional membrane structure.....	45
4.1.5. Experimental setup and operation	45
4.1.6 Characterization	48
4.2 Results	50
4.2.1 The morphology of the multifunctional membranes.....	50

4.2.2. The effect of MWCNT contents on the contact angle of multifunctional membranes	55
4.2.3. The Effect of MWCNT contents on permeation flux.....	56
4.2.4. Evaluation of multifunctional membranes performance with activated sludge.....	57
4.2.5. Antifouling property and organic removal efficiency of the multifunctional membrane	59
4.3. Conclusion.....	64
Chapter Five: Conclusions and Recommendations	66
5.1. Conclusions	66
5.2 Recommendation for future work.....	69
References	71

List of Tables

Table 2. 1 : Processing parameters for electrospinning	17
Table 3. 1: Effect of flow rate on fiber diameter, pore size and porosity. (Applied voltage= 15kV, tip to collector distance= 15cm).....	37
Table 3.2: Effect of applied voltage on fiber diameter, pore size and porosity. (flow rate=1 mL/h, tip to collector distance= 15 cm).....	38
Table 3.3: Effect of tip to collector distance on fiber diameter, pore size and porosity. (flow rate=1mL/h, applied voltage= 15kV).....	40
Table 3.4: Effect of MWCNT contents on fiber diameter, pore size and porosity. (flow rate=1mL/h, tip to collector distance= 15cm, applied voltage= 20kV)	41
Table 4. 1: Composition of synthetic wastewater.....	46

List of Figures

Figure 1. 1: (a) Conventional activated sludge process, (b) membrane bioreactor process.....	2
Figure 2. 1: Average pore size of the membranes used in different membrane process.....	9
Figure 2. 2: (a) Side-stream MBR, (b) immersed MBR.....	9
Figure 2. 3.: Phase inversion technique.....	11
Figure 2. 4.: Electrospinning Setup.....	14
Figure 2. 5: Mechanisms of membrane fouling.....	20
Figure 3. 1: Effect of flow rate on morphology and fiber diameter distribution (note: applied voltage = 15 kV, tip-to-collector distance = 15 cm) with flow rate of (a) 0.5 mL/h, (b) 1 mL/h and (c) 1.5 mL/hr. Magnification 15kX	36
Figure 3. 2: Effect of applied voltage on morphology and fiber diameter distribution (flow rate=1mL/h, tip to collector distance= 15 cm) with applied voltage (a) 15 kV, (b) 20 kV and (c) 25 kV. Magnification 15 kX.....	38
Figure 3. 3: Effect of tip to collector distance on morphology and fiber diameter distribution (applied voltage= 15kV, flow rate = 1mL/h) with tip to collector distance (a) 10cm, (b) 15cm and (c) 20cm. Magnification 15kx	39
Figure 3. 4: Effect of MWCNT contents on morphology and fiber diameter distribution (flow rate = 1 mL/h, tip to collector distance = 15 cm, applied voltage = 20 kV) with MWCNT contents (a) 0.5wt.%, (b) 1wt.% and (c) 1.5wt.%. Magnification 15kx.....	41
Figure 4. 1: Filtration Set up.....	47
Figure 4. 2: SEM micrograph of multifunctional membranes at 50X (a) open-cell foam (b) open-cell foam after ScCO ₂ and electrospun nanofiber at 500X with (c) 0 wt.%, (d) 0% MWCNT after ScCO ₂ , (e) 0.5 wt.%, (f) 0.5 wt.% MWCNT after ScCO ₂ , (g)1 wt.% (h) 1 wt.% MWCNT after ScCO ₂ , (i) 1.5 wt.% and (j) 1.5 wt.% MWCNT after ScCO ₂	51

Figure 4. 3: Thickness of the nanofibrous membrane.....	52
Figure 4. 4: SEM micrograph of the cross-section of membranes with 1% MWCNT (a) multilayer, (b) open-cell foam, (c) nanofibrous membrane; with 1.5% MWCNT (d) multilayer, (e) open-cell foam, (f) nanofibrous membrane.....	53
Figure 4. 5: SEM micrograph of the cross-section of membranes with 0% MWCNT (a) multilayer, (b) open-cell foam, (c) nanofibrous membrane; with 0.5% MWCNT (d) multilayer, (e) open-cell foam, (f) nanofibrous membrane.....	54
Figure 4. 6: Multifunctional Membranes with (a) 0 wt%, (b) 0.5 wt%, (c) 1wt% and (d) 1.5 wt% MWCNT.....	54
Figure 4.7: Water contact angle of membranes with 0 wt.%, 0.5wt.%, 1 wt.% and 1.5wt.% MWCNT.....	55
Figure 4. 8: Effect of MWCNT loadings on (a) pure water flux and (b) synthetic wastewater flux of multifunctional membranes(b)	56
Figure 4. 9: Effect of MWCNT loading on activated sludge flux for two days filtration test.	57
Figure 4. 10: Effect of MWCNT loading on activated sludge flux for (a) 5 days and (b)10 days filtration test.....	58
Figure 4. 11: Effect of MWCNT loadings on the FRR of multifunctional membranes.	59
Figure 4. 12: Effect of MWCNT loadings on the membrane retention efficiency of multifunctional membranes for (a) 5 days and (b) 10 days filtration test.	60
Figure 4. 13: Effect of MWCNT loadings on the sCOD removal efficiency of multifunctional membranes for (a) 5 days and (b) 10 days filtration test.....	61
Figure 4. 14: Multifunctional membrane after filtration with activated sludge with MWCNT loadings (a) 0 wt.%, (b)0.5 wt.% (c)1 wt.%, (d) 1.5wt.%; after cleaning the membrane the feed side with MWCNT(e) 0 wt.%, (f)0.5 wt.% (g)1 wt.%, (h) 1.5wt.%; and the permeate side with MWCNT(i) 0 wt.%, (j)0.5 wt.% (k)1 wt.%, (l) 1.5wt.%	62

Figure 4. 15: SEM micrographs of the feed side of the membranes at 500X with MWCNT loadings (a) 0 wt.%, (b)0.5 wt.% (c)1 wt.%, (d) 1.5wt.%; at 10kX with MWCNT loadings (e) 0 wt.%, (f)0.5 wt.% (g)1 wt.%, (h) 1.5wt.%.63

Figure 4. 16: SEM micrographs of the permeate side of the membranes at 500X with MWCNT loadings (a) 0 wt.%, (b)0.5 wt.% (c)1 wt.%, (d) 1.5wt.%; at 10kX with MWCNT loadings (e) 0 wt.%, (f)0.5 wt.% (g)1 wt.%, (h) 1.5wt.%.64

Figure 4. 17: SEM micrographs of the cross-section of permeate side of the membranes at 5kX with MWCNT loadings (a) 0 wt.%, (b) 0.5 wt.% (c)1 wt.%, (d) 1.5wt.%; cross-section of permeate side of the membranes with MWCNT loadings (e) 0 wt.%, (f)0.5 wt.% (g)1 wt.%, (h) 1.5wt.%.64

List of Abbreviations

PVDF	Polyvinylidene fluoride
MWCNT	Multiwalled carbon nanotube
MBR	Membrane bioreactor
MF	Microfiltration
UF	Ultrafiltration
sCOD	Soluble chemical oxygen demand
EPS	Extracellular polymeric substance
PS	Polystyrene
PU	Polyurethane
PVC	Polyvinyl chloride
SMP	Soluble microbial product
TMP	Transmembrane pressure
SEM	Scanning electron microscopy
FTIR	Fourier transform infrared spectroscopy
DMF	Dimethyl formamide
NMP	N-methyl-2-pyrrolidone
TSS	Total suspended solid

Chapter One: Preamble

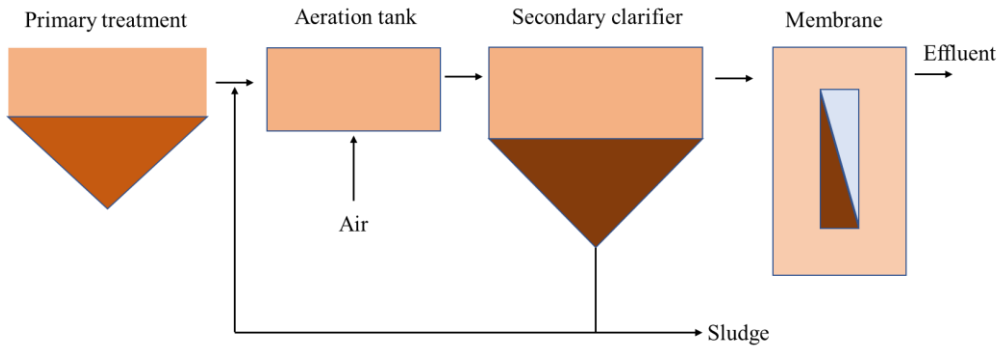
1.1. Introduction

Clean water is a basic need for human life and our ecosystem. However, rapid population growth and continuous development of the economy have resulted in the scarcity of clean water. Moreover, around 70% of the earth's surface constitutes water but the salinity for 97% of them is too high for human consumption. Among the 3% fresh water, two-third of them are in the form of glaciers and ice caps, which leaves a small quantity of accessible fresh water [1]. Due to this limited amount of fresh water, it has become a necessity to come up with alternatives for fresh water supply. Recycling water from wastewater is an emerging technology and has become an interesting research area. Wastewater treatment technologies are mainly based on physical, chemical, and biological means. However, physical, and chemical processes need high maintenance and high cost. Biological wastewater treatment is one of the best choices as it has lower operational costs, provides easy handling, and has less harmful effects on the environment.

In biological wastewater treatment, membrane bioreactor (MBR) has become a widely used process to treat wastewater over conventional bioreactor because of its low energy consumption and chemical-free operation [2]. Figure 1.1 shows the schematics of both conventional activated sludge process and two types of membrane bioreactor processes. The conventional activated sludge treatment is based on aerobic degradation of organic pollutants by biomass in an aeration tank. Consequently, the activated sludge is settled and separated from the water in a secondary clarifier while the activated sludge is recycled to the aeration tank. In contrast, membrane bioreactors combine the activated sludge process and a membrane separation process. Although the treatment is also based on aerobic degradation of organic pollutants, the biomass is retained in

a membrane. As a result, a secondary clarifier, which is an expensive facility that occupies a large area in a wastewater treatment plant, is no longer necessary. Moreover, the uses of membrane would significantly improve the effluent quality over the conventional treatment process.

(a) Conventional activated sludge process



(b) Membrane bioreactor process

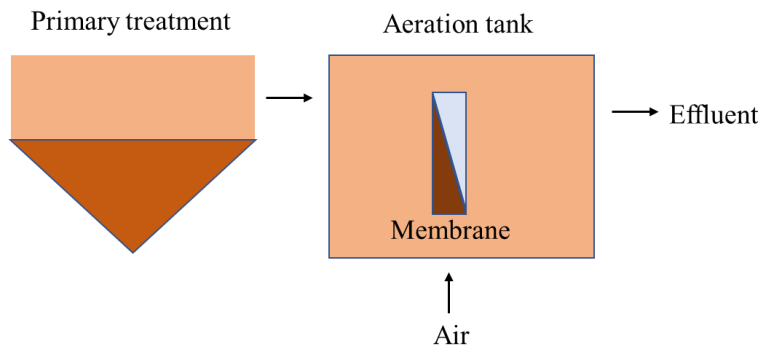


Figure 1. 1: (a) Conventional activated sludge process, (b) membrane bioreactor process

Nanofibrous membranes in membrane technology applications for water and wastewater treatment have gained interest among researchers because of their high mechanical and chemical resistance. Nanofibers possess unique characteristics such as nanoscale diameter and large aspect ratio and their surface can be modified due to their high surface to volume ratio. It has been observed that nanofibrous membranes prepared from hydrophilic polymers demonstrates better

filtration performance. Moreover, heat treatment was effective to inhibit the layered fouling on the membrane surface [3]. Electrospinning is an emerging fabrication technique to prepare nanofibers with tunable morphologies using various polymers. Nanofibrous membranes produced by electrospinning process have high pore interconnectivity and uniform pore size distribution, which would improve the filtration performance. Moreover, incorporating nanoparticles into electrospun membranes has improved the functionality (e.g., anti-microbial and anti-fouling) and the filtration performance.

1.2 Research Motivation

MBR technologies provide biological treatment integrated with membrane separation by either microfiltration (MF) or ultrafiltration (UF), where the membranes are placed either externally or inside the bioreactor [4]. Biological treatment processes help to clean wastewater suspended with soluble organics. During this process, microorganisms biodegrade complex organic materials via an oxidation reaction and the membrane separation process filters the biomass from the feed. The quality of effluent in the wastewater treatment can be evaluated by measuring the water's soluble chemical oxygen demand (sCOD), which represents the concentration of the biodegradable organic pollutants that has been removed by biological wastewater treatment [5]. However, membrane fouling is a major downside of the membrane bioreactor. Nanofibrous membranes in membrane technology applications for water and wastewater treatment have gained interest among researchers because of their high mechanical and chemical resistance. Producing novel membranes by incorporating nanomaterials has become a popular research topic due to its unique properties for fouling mitigation such as photocatalytic activity, antimicrobial activity, and hydrophilicity. Moreover, macroporous open cell foams have large specific surface area and high surface roughness, which would promote biofilm adhesion and thereby improve the organic removal

efficiency. In this study, a hybrid multifunctional membrane that integrate an antifouling nanofibrous membrane for microfiltration and an open-porous biofilm carrier for organic removal. The active surface of the membrane system is a macro-porous foam that will sustain the growth and activity of biofilm for enhanced organic removal to produce high-grade effluent. On the other hand, the incorporation of MWCNT in the electrospun nanofibrous layer would reduce the fouling of the membranes due to the ability of MWCNT to inhibit the growth of microbes and the increased hydrophilicity.

1.3. Research Objectives

The goal of this research is to develop and fabricate a multifunctional polymer-based nanofibrous membrane system that integrated a nano or micro-porous membrane and a macro-porous biofilm carrier. This study aims to utilize the advantages of the different layers of the membrane systems for wastewater treatment to achieve different functionalities to improve the performance of the membrane bioreactor. Due to the large surface area and interconnectivity among the cells, open-cell foams can be a potential habitat for microbial immobilization, which would increase the organic removal efficiency. On the other hand, the electrospun nanofibrous layer will reduce the fouling in membranes. The nanoparticles embedded in nanofibrous membranes will provide antifouling and antimicrobial effects to minimize the fouling of the membranes. The first phase of the research investigated the effects of processing parameters of electrospinning (i.e., flow rate, applied voltage, tip to collector distance) and material parameter (i.e., MWCNT loading) on the fiber diameter, pore size, and porosity of PVDF nanofibrous membranes. In the second phase of this study, the multifunctional membrane system was fabricated by integrating nanofibrous membrane layer to a polymeric macroporous open cell foam. Then, the effects of MWCNT

loading on the filtration performance and fouling behaviour of the membrane system were investigated.

1.4. Thesis structure

In Chapter one, the scarcity of clean water in the world and the importance of the biological wastewater treatment process for water recycling have been described. This chapter introduces the emerging technology of nanoparticle embedded nanofibrous membranes in the membrane bioreactors and describes the proposal of a novel multifunctional membrane with different layers to provide different functionality in the same system. The chapter concludes with the goal and objectives of the research work. Chapter two provides a detailed literature survey and reviews the background of the research. Chapter three reports an experimental investigation on the effect of processing parameters of the electrospinning process and material formulation on the morphology of the electrospun membrane. Chapter four shows the fabrication of the multilayer membranes and the effect of nanoparticles (i.e., MWCNT) on the membrane performance and the effluent quality after filtration. Chapter five concludes the results and contributions of this research and suggests some potential future works for this research.

Chapter Two: Background and Literature Review

This chapter reviews the membrane applications and attached growth processes in biological wastewater treatment. Then, different manufacturing processes for the polymeric membrane and foam fabrication were discussed. It also provides a summary of the effects of processing parameters and material formulation on the morphology of membranes fabricated by electrospinning. In addition, this chapter describes the fouling in membranes in biological wastewater treatment and reviews the factors that affect the fouling behaviors.

2.1. Biological Wastewater Treatment

Biological wastewater treatment is an important technology used in some wastewater treatment plant that help to clean the wastewater suspended with soluble organics. During this process, microorganisms biodegrade the complex organic materials via oxidation reaction and transform them into acceptable products. Microorganisms present in the wastewater use organic materials as an energy source to produce new microbial cells. Soluble chemical oxygen demand (sCOD) represents the concentration of the biodegradable organic pollutants that can be removed by biological wastewater treatment [6]. Biological wastewater treatment process is advantageous over other treatment processes such as chemical and physical processes due to its lower demand of capital investment, more environmentally sustainable, and lower operating costs. Biological wastewater treatment processes can be categorized into three major types; suspended growth, attached growth (biofilm), and hybrid growth system.

In suspended growth technology, microorganisms present in the mixed liquor biodegrade the pollutants of the wastewater. Conventional bioreactor and MBR both worked based on the principle of suspended growth technology. The details of the MBR will be discussed in the later

section of this chapter. In conventional bioreactor, the wastewater treatment process went through three different stages: primary, secondary, and tertiary. In the primary stage, large debris and grits are removed from the wastewater by mechanical screening. The secondary treatment process removes the dissolved organic material and convert the colloidal material to a biological sludge, which rapidly settles in the secondary clarifier. This process is known as activated sludge process. Then, the water moves to the physical separation process for filtration in tertiary stage. In attached growth systems, support media are used for the immobilization of microorganisms and to sustain the growth of biofilm. Biofilm can be defined as an assemblage of immobile microbial cells attached to a surface or to each other, entrapped in a matrix of self-produced extracellular polymeric substance (EPS). These biofilms act as a shelter and increase the settleability of the bacterial colonies. [7]. Trickling filter is a common attached growth system, where a moving bed with supporting media is used for the formation and growth of biofilm. This support media consists of rock, gravel, coke, polymer foam, ceramic, or plastic media. In hybrid growth system, both suspended growth and attached growth systems are applied for organic removal. The suspended biomass and the biofilm attached to the support media can maintain high biomass concentration. Support media, depending on the size of the supporting media, can either be firmly attached to the tank or kept in free motion with the activated sludge. Higher accumulation of microorganism in the biofilm enhances the biomass concentration, which results in higher organic removal efficiency in the system. In this system, the uses of support media to immobilize biomass eliminate the needs to use the secondary clarifier to separate the solid from the water. This would reduce the required space of the wastewater treatment plant [8].

2.2 Membrane Applications in Biological Wastewater Treatment

Membranes can be defined as separating media for two distinct phases. It acts as a selective barrier that will allow the passage of certain constituents and retain other constituents in the liquid. Membrane filtration is used in different industrial applications including the chemical industry, dairy industry, sugar industry, and pharmaceutical industry. In the filtration process, the size of particles being filtered is extended to include dissolved constituents (i.e., typically from 0.1 nm to 10 μm). Membrane technology can be classified based on the size of particles being filtered and the separation principle. Figure 2.1 summarizes the targeted particle sizes in different membrane technologies. Some of the main technologies include microfiltration (MF), ultrafiltration (UF), nanofiltration (NF), reverse osmosis (RO), and membrane distillation (MD). Among these different technologies, MF, UF, NF and RO are pressure driven membrane processes, which applies pressure on the feed side to separate the particles from the permeated stream, but RO differs from MF, UF and NF in the mechanism of fluid flow [4]. The flow is governed by the osmosis across the membrane. It is commonly used to remove salts and other particles from sea water to get pure drinking water. MF, UF, and NF are based on the same principles but are targeted for different particle sizes. MD is a thermally driven separation process assisted by the phase separation. The driving force for this process is partial vapor pressure difference commonly triggered by the difference in temperature.

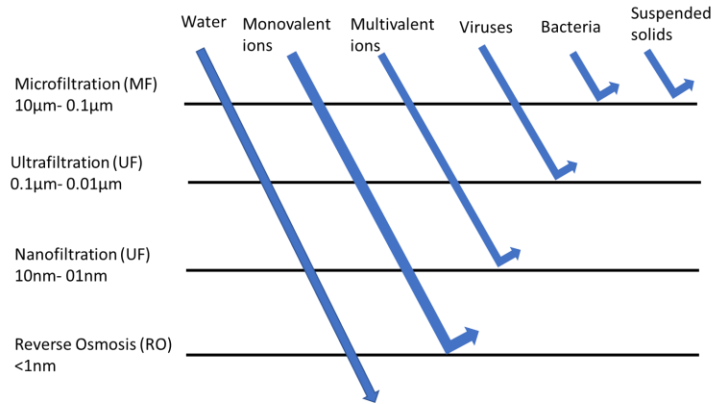


Figure 2. 1: Average pore size of the membranes used in different membrane process

In biological wastewater treatment processes, membranes can also be used in bioreactors to separate particles and biomass from the water. This technology is commonly known as membrane bioreactors (MBR), which combine biological wastewater treatment and membrane separation using MF or UF. In MBR, after the primary stage, membranes are used to filter the biomass from the feed along with the activated sludge process. This replaces the application of the secondary clarifiers and also eliminates the tertiary stage. In MBR, the membranes are placed either externally (i.e., side-stream MBR) or inside the bioreactor (i.e., immersed MBR). Figure 2.2 illustrates the side-stream MBR and the immersed MBR. MF and UF membranes are used in MBRs due to their larger pores to get higher permeation flux [5]. Moreover, MF and UF can filter the viruses, bacteria, and colloidal particles from the wastewater. The pore size ranges from 0.1 to 10 μm in MF and from 0.01 to 0.1 μm in UF. Multitube membranes are used in side-stream MBRs while flat sheet or hollow fiber membranes are used in immersed MBRs [9].

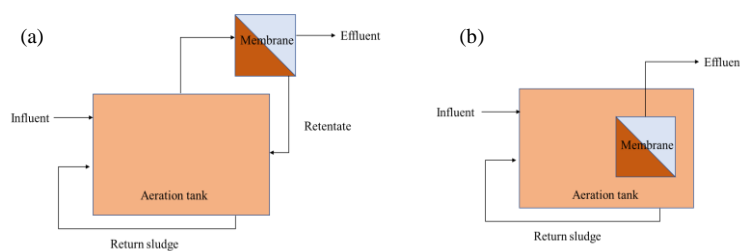


Figure 2. 2: (a) Side-stream MBR, (b) immersed MBR

2.3. Membrane fabrication methods

The fabrication technique adopted to produce polymeric membranes depends on the polymer type and the desired membrane morphology. The most commonly used techniques to fabricate polymeric membranes include phase inversion, interfacial polymerization, stretching, track-etching, and electrospinning.

2.3.1. Phase Inversion process

Phase inversion is the most extensively used process to fabricate polymeric membranes. This process transforms homogeneous polymer solution in a controlled manner from liquid to solid [10]. In this technique, the homogeneous polymer solution is casted on a flat substrate by using the doctor blade technique. The transformation can be achieved in several ways, such as (i) immersion precipitation, (ii) thermally induced phase separation (iii) evaporation induced phase separation and (iv) vapor induced phase separation. In immersion precipitation process, the polymer solution is immersed in a non-solvent coagulation bath, usually water. Demixing and precipitation occur due to the solvent and non-solvent exchange. The solvent and non-solvent must be miscible. The chemical nature and the concentration of the polymer is very important in this process. Increasing polymer concentration produces membrane with lower porosity and smaller pore size. Casting solution with polymer concentration with a range 12-20wt.% produces UF membranes [11]. Figure 2.3 shows a schematic of the immersion precipitation process. Thermally induced phase separation is based on changing temperature to induce the demixing of the homogenous polymer solution to form a multiphase system. During the demixing process, the homogeneous solution separates into a polymer rich and polymer deficient phase. In evaporation induced phase separation, a viscous polymer solution is prepared in a mixture of solvent and non-

solvent. Then, the polymer solution is casted on a flat substrate and a thin polymer film is formed by the complete evaporation of the solvent and the non-solvent from the casted solution. In vapor induced phase separation, the polymer solution is kept to an atmosphere containing a non-solvent (e.g., humid air) and the demixing or precipitation occurs due to the absorption of water from the non-solvent into the solution. Among these fabrication techniques, immersion precipitation and thermally induced phase separation are the most widely used methods to fabricate polymeric membranes [12].

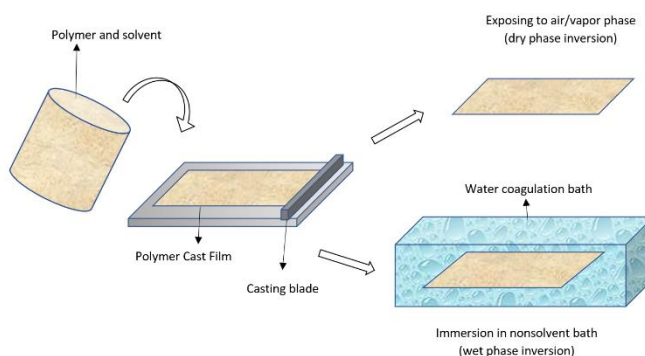


Figure 2. 3.: Phase inversion technique

2.3.2. *Interfacial polymerization*

Interfacial polymerization (IP) is the most accepted method to fabricate thin film composite (TFC) RO and NF membranes. The first interfacial polymerized TFC membrane was developed by Cadotte et al. [13] and regarded as a breakthrough in membrane performance. The original IP protocol involved the following steps, the microporous polysulfone support soak in an aqueous solution of a polymer amine. Then, the amine impregnated membrane is immersed in the solution of diisocyanate in hexane. Finally, the polymer is cross-linked after heat treated at 110°C. There are various factors that affect the morphology and composition of the membrane. These include

polymer concentration, reaction time, solvent type, and post treatment condition [14-16]. Novel monomers such as p-phenylenediamine, piperazine, triethylenetetramine, N-N'-diaminopiperazine, N-(2-aminoethyl)-piperazine, and poly(ethyleneimine) are gaining popularity for the preparation of TFC membrane by the IP process. These monomers contain functional groups such as hydroxyl, carbonyl, carboxyl that improve hydrophilicity and antifouling property of the membranes [17,18]. Another improvement has been done by adding an active organic modifier into the solution, which can participate in the reaction and provide functional barrier that improves the antifouling property of RO membrane [19].

2.3.3 Stretching

Microporous membranes that are used in MF, UF and MD are manufactured by extrusion followed by stretching technique. Stretching was used to fabricate polymer membrane in 1970 and its proprietary was owned by the company Celgard®. Polyethylene (PE) and polypropylene (PP) based membranes were produced to use in energy storage devices by Celgard® [20]. It is a solvent free technique, and the polymer is heated above the melting point and extruded into thin sheet. Then the extruded sheet is then being stretched to get microporous structure [21]. The stretching process is generally conducted in two steps: cold stretching, and hot stretching. Pores are nucleated by cold stretching followed by hot stretching to control the final pore structure of the membranes. Hot stretching controls the final pore structure by enlarging the pore size. During hot stretching the temperature is set between the glass transition temperature (T_g) and melting temperature (T_m) of PP to induce chain extension and orientation of polymer chain. Highly crystalline polymers are more suitable for this fabrication process, where the crystalline region of the polymers offers strength, and the amorphous regions allows the formation of the porous structure.

2.3.4. Track etching

In this fabrication process, energetic heavy ions irradiate the non-porous polymeric films to form a linear damaged track across the film [22]. The advantage of this technique is that it has precise control on the pore size distribution, ranging from nanometers to tens of micrometers. The pore sizes and their distribution determine the water transport property of the membrane. The membrane porosity can be controlled by the duration of irradiation time and the pore size can be determined by the etching time and the processing temperature. Porous polyethylene naphthalate (PET) films developed by Komaki *et al.* [23] were irradiated by fission fragments, which were acquired from thermal neutron fission of uranium-235. Polycarbonate (PC) and PE are the most commonly used polymers in track etching due to their stability towards organic solvents and acids. PVDF and its copolymers had been investigated to be used in track etching, but they showed resistance towards strong oxidizers, which resulted in longer processing time to form pores [24].

2.3.5 Electrospinning

Electrospinning is relatively new and is becoming popular to develop polymeric nanofibrous membranes. Compared to traditional phase inversion techniques for membrane fabrication, electrospinning allows the formation of interconnected pores with uniform pore size and porosities exceeding 90%. The unique characteristics of electrospun membranes such as micro and nano structural characteristics, high surface area, high porosity, and high orientation of nanofibers have made it a competitive option for several applications including energy storage, health care, biotechnology as well as environmental applications [3]. In electrospinning, high electric voltage is applied to generate nanofibers from a charged polymer solution. A schematic of electrospinning setup is shown in Figure 2.4

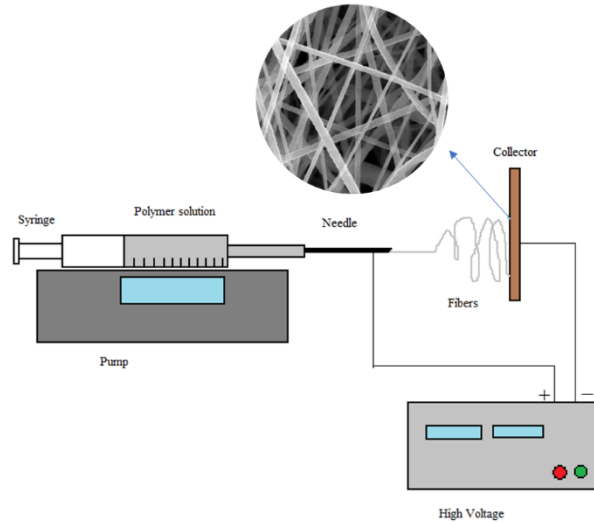


Figure 2. 4.: Electrospinning Setup

Electrospun membranes are composed of overlapped nanofibers with diameter in nanometer scale. When the electrostatic force is greater than the surface tension of the solution, a charged fluid jet is produced. The solvent then evaporates and leaves behind the polymer fibers deposited on a grounded collector. Highly porous structure of smooth, defect-free non-woven nanofibrous membrane can be produced by varying the operating conditions and solution parameters [25]. The effects of processing parameters of electrospinning on the morphology and the properties of the nanofibers will be discussed later in this chapter.

2.4. Foam

Foam can be defined a solid or liquid phase consists of numerous gas voids. A wide variety of material properties can be achieved by changing the cell size, cell population density, and cell size distribution in the foams. Polymer foams can be classified into closed-cell foams and open-cell foam based on their cellular structures. Closed-cell foams consist of discrete gas pockets separated

by cell walls. In contrast, open-cell foams have interconnected pores establishing a continuous porous network structure. In general, open-cell foams contain 80-90 vol% of open-cell structure whereas the closed cell foam contains less than 10 vol.% open-cell structure [26].

Polymeric foams have been used in a variety of applications including thermal packaging, acoustic insulation, energy dissipation, shock protection, filtration, and separation. PVDF, PP, PE, polystyrene (PS), polyurethane (PU), and polyvinyl chloride (PVC) are commonly used polymers to fabricate polymeric foams due to their suitable melt rheology [27]. Open-cell foam possesses unique properties such as lightweight, open porosity, impact absorption, floatation and acoustic insulation. Open-cell foams can also be used in wastewater technology as a potential habitat for microbial immobilization due to their large surface areas [28].

2.4.1 Open-cell foam fabrication methods

With the ongoing developments of open-cell foams and their extensive applications in different fields, researchers have investigated different fabrication methods. The techniques used to fabricate open-cell foams are discussed in the following section.

2.4.1.1 Thermally induced phase separation

Thermally induced phase separation (TIPS) is a straightforward process to fabricate polymeric foams and the morphological characteristics such as, pore size, porosity and interconnectivity can be controlled. Similar to TIPS used in membrane fabrication, this method is based on the de-mixing of a homogeneous polymer solution by the change of temperature. In this process, phase separation occurs by cooling a homogeneous polymer solution and then the solution separates into polymer rich and a polymer deficient phase. After this step, the porous polymeric structure is obtained by removing the solvent [29]. During this process, polymer foams may shrink; however, it can be

avoided by using freeze drying, supercritical drying, or vacuum drying. In TIPS, the morphology of microporous foams can be tailored by tuning the thermodynamic and kinetic parameters [30].

2.4.1.2. Emulsion freeze drying

In emulsion freeze drying process, an emulsion is created by the homogenization of polymer solvent and water. After that, the emulsion is cooled rapidly to freeze the structure, followed by the removal of the solvent and water using freeze-drying. It is very important to control the various processing factors (e.g., volume fraction of the dispersed phase and emulsion stability) to create an emulsion of two immiscible phases, where the continuous phase is a polymer rich solution and the dispersed phase is water. Moreover, emulsion stability can affect the pore size and the uniformity of the pore structure as emulsion are not usually thermodynamically stable system [31].

2.4.1.3. Particulate leaching

In particulate leaching method, solid particles such as sodium chloride or potassium chloride crystals are added into a polymer matrix. Then, a porous cellular structure is formed throughout the polymer matrix as the particles dissolved out of the polymer matrix by using a solvent. Usually, compression molding is used to prepare the sample before the leaching process. This technology has commonly been used to fabricate highly porous bio-scaffolds [32].

2.5. Effect of processing parameter on electrospinning

In electrospinning process, solutions properties such as polymer molecular weight, viscosity, and concentration directly affects the fiber properties. Conductivity of polymer solution can also alter the fiber properties. Fiber properties can be affected by operating conditions such as applied voltage, solution flow rate, and tip-to-collector distance. Ambient conditions such as temperature and humidity of the electrospinning chamber can also affect fiber morphology. Porosity, pore size

distribution, hydrophobicity, and surface morphology of the electrospun mats are controlled by the fiber diameter and the morphology [33]. Therefore, it is essential to understand the characteristics of nanofiber as a function of processing parameters.

Table 2. 1 : Processing parameters for electrospinning

Solution Parameters	Process Parameters	Environmental Conditions
Concentration	Electrostatic Potential	Temperature
Viscosity	Electric Field Strength	Humidity
Surface tension	Electrostatic field shape	Local atmosphere flow
Conductivity	Working distance	Atmospheric compositions
Dielectric constant	Feed rate	Pressure
Solvent volatility	Orifice Diameter	

2.5.1. Applied Voltage

The level of applied voltage to the polymer solution is a critical parameter in the electrospinning process. Fiber formation occurs only after reaching a threshold voltage, which causes instability in the polymer jet to form a Taylor cone at the needle tip. Contradictory observation on the effect

of applied voltage on the fiber diameter in the electrospinning process had been reported in literatures. On the one hand, it has been shown that higher applied voltage can increase the acceleration of the jet, and thereby lowers the flight time. In this case, the fibers will not get enough time to stretch and elongate before getting deposited and lead to increased fiber diameter [34]. On the other hand, it was also found that increasing the applied voltage results in high electric field strength, which increases the electrostatic force on the polymer jet resulting in thinner fibers [35]. According to literature, in most cases a higher voltage produces fibers of thinner diameter as it causes greater stretching of polymer jet [36]. Higher voltage can increase the probability of bead formation on the nanofiber string. When the voltage is increased, the volume of the drop at the tip decreased which caused the Taylor cone to narrow down. The jet originated from the liquid surface within the tip formed beads [37]. Therefore, it is evident that applied voltage is an important parameter to control the morphology of the nanofibrous membrane.

2.5.2 Flow rate of polymer solution

The flow rate of polymer solution in electrospinning can affect the morphology of the electrospun fibers. It is a crucial processing parameter that can influence the jet velocity and material transfer rate. A lower flow rate is preferable as the solvent will get enough time for evaporation [38]. Yuan *et al.* [38] found that increasing the flow rate of PS solution increases fiber diameter and pore size. Higher flow rate provides higher volume of polymer jet, which result in larger fiber diameter. In addition, few studies showed the formation of beaded fiber with high flow rates due to the unavailability of proper drying time before reaching to the collector [39-40]. Therefore, the flow rate of the solution should be selected in a way that the solvent gets enough time for evaporation before reaching to the collector to avoid the formation of beads in the fibers.

2.5.3. Tip-to-collector separation distance

The distance between the tip and the collector is an importance processing parameter to control the fiber morphology and the diameter. It is necessary to maintain a minimum distance between the tip and the collector so that the fibers will get enough time to dry before getting deposited onto the collector. It has been observed that beads are formed when the distances are either too close or too far, as the tip-to-collector distance has direct influence on the jet flight time and electric field strength [41-42]. It has been mentioned earlier in this chapter that lower flight time increase the possibility of getting beaded fibers. Buchko *et al.* [43] showed that flatter fibers can be produced at shorter distances whereas rounder fibers can be formed with longer distance rounder. In another study [44], it has been found that closer distance between the tip and the collector formed fibers of smaller diameters. From these studies, it has been observed that tip-to-collector distance can affect the shape of the fibers and fiber diameter. Therefore, an optimum distance should be maintained between the tip and the collector for the complete evaporation of the solvent from the nanofibers.

2.6. Fouling in membranes

Membrane fouling is a major downside of the MBR. It badly affects the membrane performance by reducing the permeate flux when the MBR is operated at constant transmembrane pressure (TMP) or by increasing the required TMP to maintain at constant permeate flux. It deteriorates the filtration performance that results in high maintenance and high operating costs [45]. The economic feasibility of MBRs depends on the permeate flux, which is affected by the effective fouling. Membrane fouling occurs due to the interaction between membrane material and particles, colloids, and sludge flocs. Fouling mechanism can be described by pore narrowing, pore clogging, and cake formation. Figure 2.5 shows the fouling mechanism in membranes. Pore narrowing

happens by the adhesion of soluble microbial product (SMP) on the walls of pores. This decreases the pore size of the membrane. Then, in the next stage, known as pore clogging, TMP rises exponentially due to biofilm formation and pore blocking [46]. Finally, the cake layer formed by continuous accumulation of microorganisms, biopolymers, and inorganic matter on the membrane surface [47]. In this stage, sudden increase of TMP indicates the severe fouling in the membranes. Due to oxygen limitation, the bacteria inside the biofilm tends to die and thereby produces more EPS and causes severe fouling [48]. Membrane cleaning is necessary at this stage. It is essential to reduce the membrane cleaning frequency by delaying the final stage in order to reduce the operational cost of the MBRs.

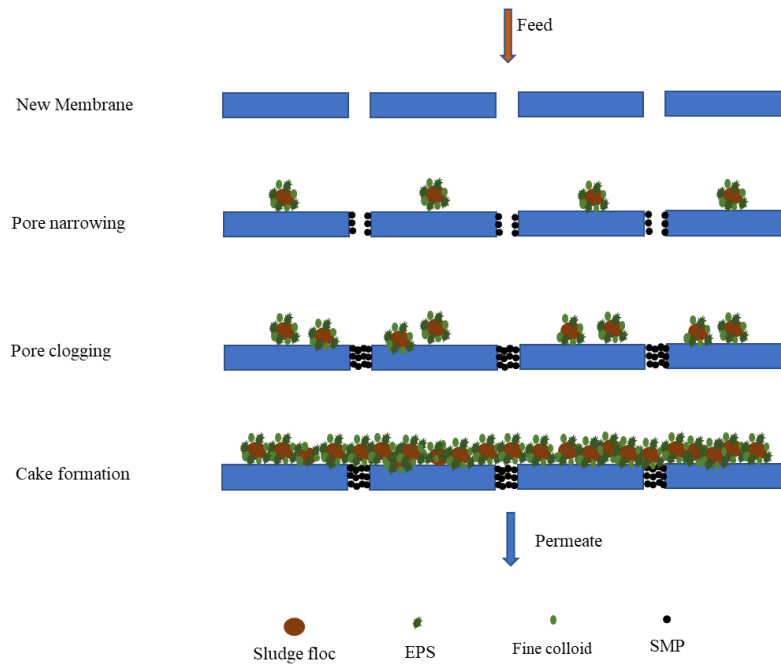


Figure 2. 5: Mechanisms of membrane fouling

2.6.1. Classification of foulants

Based on the biological and chemical characteristics, membrane foulants can be categorized into biofoulants, organic foulants, and inorganic foulants [49].

2.6.1.1 Biofoulants

Biofouling is defined as the attachment, growth and metabolism of microorganisms on the membrane surface [45]. Initially, the bacteria attach to the membrane surface or inside the open pores and then they started to grow and aggregate into cluster of cells, leading to the formation of bio-cake, which affect the permeability of membranes [50]. Biofouling is a major issue for low pressure driven MF and UF membranes, as most microbial flocs in MBRs are much larger than the membrane pore size [45]. Membrane biofouling is a two-step process. In the first step, the microorganisms attach to the membrane surface through weak Van-der-wall forces. Then, their growth and multiplication on the membrane surface cause biofouling [51]. This bio-cake layer consists significant amounts of bacteria, microorganisms and biomolecules [52]. It can be anticipated that deposited and attached cell would behave differently from the suspended cells due to their different community structures [53]. Besides, the reduced dissolved oxygen (DO) and substrates in the biofilm matrix can affect the growth and metabolism of some bacterial species. In some cases, the live cells change their gene expression to adapt to community-based state [54]. The EPS produced by the cells can provide the mechanical stability of the biofilm and can provide better cell-cell interactions [55]. Though biofoulants on the membrane surface causes flux reduction, their presence in the bioreactor increases the organic removal efficiency as discussed earlier in this chapter.

The bacteria cells deposited on the membrane surface can be visualized by techniques such as scanning electron microscopy (SEM), confocal laser scanning microscopy (CLSM), atomic force microscopy (AFM), and direct observation through membrane (DOTM). DOTM and CLSM are widely used for the characterization of membrane biofouling [56-58-61]. CLSM is a robust technology for membrane biofouling characterization that can locate the deposited cells as well as the 3D structure of the fouling layer. Ng *et al.* [59] showed the presence of bacteria on the fouled membrane by applying CLSM to analyze the bacterial distribution on the membrane surface. The effect of biofilm structure on the membrane permeability in MBRs for dye wastewater treatment had been investigated by Yun *et al.* [60] and they found that the membrane permeability was related to the structural properties of biofilm such as porosity and biovolume. These characterization techniques to visualize the biofouling help to understand the biological flocs deposition process and the structure and architecture of the bio-cake layer.

2.6.1.2. Organic foulants

Organic fouling refers to the deposition of SMP and EPS produced by the biological activities and the deposition of dissolved and colloidal components on the membrane surface [45, 61, 62]. EPS are made up of various polymers produced by the bacteria cells. They are composed of different types of macromolecules such as polysaccharides, proteins, nucleic acids, and other polymeric substances that have been found at or outside the cell surfaces and in the intercellular space of microbial aggregates [63]. SMP are EPS that are released from the microbial aggregates into the water phase [64]. Both EPS and SMP are responsible in different ways for fouling in MBRs and affect the membrane permeability. Metzger *et al.* [65] investigated the composition of the fouling layers and their effects on the MBRs. After filtration, the fouling layers were categorized into upper layer, intermittent layer, and lower layers by respectively doing rinsing, backwashing and

chemical cleaning. The results revealed that the upper fouling layer had porous, loosely bound cake layer with a similar composition to the sludge flocs. The intermittent layer was composed of equal amount of SMP and bacteria aggregates and a high concentration of polysaccharides. The lower layer was largely composed by SMP. This layer had a higher concentration of soluble bound proteins. This study showed the distribution of biopolymers on the membrane surface. In another study, Wang *et al.* [66] investigated the formation process and fouling behavior of dynamic membranes and self-forming dynamic membrane bioreactor. They found that the organic removal efficiency gained the value as high as 80% with the modified self-forming dynamic membrane bioreactors.

The effective techniques for identification and characterization of organic fouling in MBRs are Fourier transform infrared spectroscopy (FTIR), solid state ^{13}C -nuclear magnetic resonance (NMR) spectroscopy and high-performance size exclusion chromatography (HP-SEC). Zhou *et al.* [67] showed that by doing FTIR, spectra of biopolymers, considerable amounts of them were identified as proteins and polysaccharides. In another study, C-NMR analysis by Kimura *et al.* [68] revealed that the foulants were rich in proteins and polysaccharides. The high polysaccharides concentrations in sludge supernatant are responsible for high fouling rates [69].

2.6.1.3. Inorganic fouling

Inorganic fouling occurs in by either chemical precipitation or biological precipitation. The chemical precipitation occurs due to the concentration polarization, which happens when the chemical species exceeds the saturation concentration. Due to the elastic nature of biofilm or the bio-cake, they can protect the surface layer from shear stress and resulted in greater degree of concentration polarization and precipitation of organics [70]. Membrane scaling can be increased

by the presence of carbonates of metals such as Ca, Mg and Fe [71]. Biological precipitation is another reason for inorganic fouling. Ionizable groups present in biopolymers such as COO^- , CO_3^{2-} , SO_4^{2-} , PO_4^{3-} , OH^- can easily capture metal ions. Metal ions can form complexes and form a dense cake layer that affects the flux [72]. Though inorganic fouling is a problem in MBRs, a small amount of metals such as calcium can improve the membrane permeation by its positive effect on sludge flocculation ability [73].

2.7. Factors effecting membrane fouling

Factors affecting membrane fouling can be categorized into three parts: membrane characteristics, operating conditions, as well as feed and biomass characteristics. The effects of membrane characteristics on fouling are briefly discussed below.

2.7.1. Membrane material

The membrane material has a significant effect on the fouling property of the membranes. Membranes can be classified into three categories based on the membrane materials: ceramic, polymeric and composite membranes. Ceramic membranes showed excellent filtration performance because of their high chemical resistance, inert nature, and hydrophilic nature [74] but their high cost of manufacturing and fragile nature make them economically not viable for MBR applications [65]. Polymeric membranes are widely used due to their good physical and chemical resistance and ease of fabrication; however, due to their hydrophobic nature, they tend to foul more easily [74]. Composite membranes are fabricated from two or more materials to combine the properties in the products to mitigate fouling. Therefore, recent research is mainly focused on reducing membrane fouling by modifying the membrane materials.

Previously cellulose, ethyl cellulose and cellulose acetate (CA) obtained from natural resources were used in commercial membranes because of their low cost. But their low chemical resistance has made them less attractive and are being replaced by synthetic polymers [3]. Polymers such as PVDF, PES, polysulfone (PSf) and polyacrylonitrile (PAN) are mostly used in membrane technology because of their good mechanical strength and chemical resistance, easier fabrication process and low cost. But the polymer membranes suffer from fouling due to their hydrophobic characteristics [75]. Membrane materials play an important role in membrane fouling and it depends on the pore size, morphology, and hydrophobicity. The fouling behavior of the membranes can be determined by the affinity between the EPS/SMP and the membrane surface. Zhang et al. (2008) [76] studied the adsorptive fouling of EPS with different polymeric membranes and found that the adsorptive fouling degrees of the three membranes were in the order of: PAN < PVDF < PES. This indicated that membrane properties such as hydrophilicity might play an important role in adsorbing EPS, eventually causing different adsorption capacities. Since the PAN membrane used in this study was the most hydrophilic, the adsorptive fouling of PAN was much less than those of PES and PVDF membranes. Common polymers that are being used in different studies for antifouling membrane fabrication is discussed below.

2.7.1.1. Polyvinylidene fluoride membranes

PVDF is a semicrystalline polymer with repeated units of $-(\text{CH}_2\text{CF}_2)_n-$. PVDF is being used by researchers and manufacturers in recent years due to its good properties such as high mechanical strength, chemical resistance, and good thermal stability. It is also soluble in some common solvents such as N, N-dimethylacetamide (DMAc), dimethyl formamide (DMF), and N-methyl-2-pyrrolidone (NMP). PVDF membranes can be prepared by vapor induced phase separation (VIPS), solution casting, electrospinning, etc. PVDF has different polymorphs among which α phase and

β phase are the most common ones. The α -phase is the most common and stable polymorph of PVDF, while the β -phase is the most important one due to its piezoelectric and pyroelectric properties. The amount of PVDF β crystal, can be increased by mechanical stretching, shearing, co-polymerization, crystallization under high pressure, electrospinning, and crystallization in polar solvent. Zheng *et al.*, 2007 [77] showed that by controlling electrospinning parameters PVDF fibrous membranes containing mainly α - or β - or γ -phase could be fabricated successfully. It was found that an increase in β -phase content was observed by adding a solvent with a low boiling point. Decreasing the electrospinning temperature, decreasing the feeding rate and tip-to-collector distance can all bring about an increase in β -phase content. The β -phase contains all trans linkages where hydrogen atoms oppose fluorine atoms, giving it the highest dipole moment per monomer unit of all PVDF phases. In a recent work of Huang *et al.* [78], it has been observed that after liquid quenching and annealing above the glass transition temperature, the highest amount of β phase PVDF was obtained in the PVDF/polyethyl methacrylate (PEMA) (3:2) blend with a crystallinity of β phase at around 28% [79]. Piezoelectric electrospun membrane shows high potential for water treatment. The electroactive membranes showed a stable flux with low TMP at the time of continuous filtration of synthetic biofouling solutions [77]. These membranes have been shown to reduce the initial rate of fouling by preventing fouling deposition and cake layer formation. In this study, among other solvents used in fabrication (e.g., DMSO, NMP, and DMF) DMF gives the best result as a solvent for the nanofiber fabrication and filtration. Due to the outstanding properties such as good chemical resistance, good thermal properties, high mechanical strength and solubility in common solvents makes PVDF a good candidate for membrane fabrication.

2.7.1.2. Polyethersulfone in membranes

PES is another polymer, which is an excellent choice for membrane preparation owing to its mechanical, chemical, electrical and thermal properties and a high degree of flexibility. PES is one of the high-temperature engineering thermoplastics in the polysulfone family. It is an amorphous, transparent thermoplastic. But because of the hydrophobic nature PES membranes has greater tendency for fouling. The disadvantages of PES can be alleviated by blending PES with organic and inorganic materials. These composite PES membranes can be used at high temperature, under a wide range of pH, in a sterilized condition for pharmaceutical applications, for protein recovery, wastewater treatment and other separation processes [80]. To improve the hydrophilicity and antifouling ability of membrane, blending pre- developed nanoparticles with the polymer is a common method.

UF membrane prepared by PES and iron-tannin-framework (ITF) complex exhibited high water permeability, bovine serum albumin (BSA) rejection and superior antifouling ability. Moreover, the addition of ITF complex enhanced the hydrophilicity and porosity of the membrane [81]. ITF complexes are built from iron ion and tannin acid (TA). The phenolic hydroxyl groups on the surface of the TA, improves the hydrophilicity of the PES membrane. PES with 0.3% ITF complex shows flux recovery (FRR about 66.1%) whereas pristine PES membrane shows FRR value of 88.3% for BSA solution. Zinc oxide nanoparticles, graphene oxide- zinc oxide (GO-ZnO) nanohybrid and amino functionalized multi-walled carbon nanotubes (NH₂-MWCNTs) [82-85] have been utilized with PES polymer to improve the hydrophilicity and antifouling property of the ultrafiltration membrane. The addition of NH₂ modified MWCNT showed good compatibility with PES polymer matrix. With 0.1% NH₂-MWCNT gives highest pure water flux, BSA rejection and flux recovery ratio of 89.7% with excellent antibiofouling property [85].

2.7.1.3. Polysulfone in membranes

PSf is a thermoplastic polymer that has been widely used in membrane processes because of its desirable thermal and mechanical properties, and its chemical stability; however, fouling occurs in the membranes due to its hydrophobic nature. Various approaches have been taken in order to overcome the biofouling problem. These include plasma treatment, amphiphilic grafting of copolymer, and modification of the membrane surface by a chemical reaction with hydrophilic components [86].

It has been mentioned earlier that electrospun nanofibrous membranes have a great potential for membrane technology due to their high porosity and interconnected pores; however, their low mechanical strength and difficulty in handling are the major disadvantages [87]. There are many methods to overcome these issues: addition of nanoparticles, heat treatment, hot pressing, polymer blending, plasticization and cross-linking [88]. Applying heat treatment is an environment-friendly process to modify the polymer membranes. Arribas, P *et al.* [86] developed PSf electrospun membranes and applied heat treatment to improve their properties. In their work, heat post treatment (HPT) (i.e., heating the membrane between the glass transition temperature and the melting temperature of the electrospun polymer) was applied to tune the morphological and structural properties of the membrane and upgrade the filtration performance. Compared to a commercially used PSf based microfiltration membrane (HPWP, Millipore), the heat-treated membrane showed higher filtration performance. The higher permeability of the fabricated PSf membrane than the commercial PSf membrane allows it to be used at lower pressure, resulting in reduced energy consumptions. Their findings confirm the structural advantages of the electrospun membranes over the traditional membranes for their three-dimensional interconnectivity among pores and high void fractions (i.e., higher porosity leads to more channels for water flow).

Moreover, shorter manufacturing time makes it a potential candidate to use it in MF application and lessen the overall cost of the system.

2.7.1.4. Polyacrylonitrile in membranes

PAN is a semicrystalline organic polymer with the formula $(C_3H_3N)_n$ and has a nitrile (CN) functional group attached on the PE backbone as the unit structure. PAN has been used in membrane processes because of its hydrophilic nature, high mechanical and thermal stability, superior mechanical properties. It is soluble in dioxanone, ethylene carbonate, DMSO, chloroacetonitrile, dimethyl phosphite, dimethyl sulfone, sulfuric acid, nitric acid, and DMF [89-90]. Incorporating nanomaterials in polymeric membranes for water and wastewater treatment have become popular research topic to mitigate fouling. The nanofibrous PAN membranes were prepared with fumarate- alumoxane (Fum-A) nanoparticles via electrospinning process by Moradi *et al.* [89] for MBR applications. Fumarate alumoxane nanoparticle has covalently bound hydroxyl and carboxylate group on its surface [91]. By blending Fum-A nanoparticle with PAN polymer spinning solution, the hydrophilicity and water permeability improved significantly. From the results obtained from their research, it has been revealed that with 2 wt.% Fum-A, the membranes exhibited the highest FRR value of 96% with lowest irreversible fouling of 4% for filtration of activated sludge suspension. However, higher Fum-A nanoparticles concentrations causes agglomeration of nanoparticles and leads to pore minimization, which ceases the pure water flux of the membranes. After that, Moradi *et al.* [92] prepared a novel microfiltration membrane with citrate-para-aminobenzoate alumoxane (PC-PABA) nanoparticles with PAN by electrospinning process. Citric acid (CA) has been chosen as they provide hydrogen bonding and other bonding site for conjugation to other molecules [93]. The presence of hydrophilic citrate alumoxane, carboxylate and hydroxyl groups in PC-PABA improved the hydrophilicity of the membranes. 3

wt.% of PC-PABA loaded PAN membranes gave the highest FRR value of 98.1% during activated sludge filtration and showed outstanding durability in long term filtration. In recent years, many research works are focused on incorporation of nanoparticles as a functional agent with polymers to improve the performance of the membranes by taking the advantages of the unique properties of the nanoparticles.

2.7.2. Hydrophilicity and hydrophobicity of membranes

Hydrophilicity and hydrophobicity of a membrane can be characterized by measuring the contact angle of a water droplet on the membrane surface. It shows the affinity of water to the membrane surface. Larger contact angle indicates higher hydrophobicity of the membrane [94]. If the water contact angle is larger than 90, the membrane surface is considered to be hydrophobic. In contrast, if the water contact angle is smaller than 90, the membrane surface is considered to be hydrophilic. The contact angle of membranes is related to the morphology of the membrane surface and the pore size of the membrane. Hydrophilic membranes show better anti-fouling performance compared to hydrophobic membranes. Hydrophobic membranes are more likely to foul due to the hydrophobic interaction between feed water, microbial cells, and membrane material [95]. It has been found that in hydrophobic MBRs, more polysaccharides and protein are rejected due to the cake layer formation, which results in lower permeability [96]. It should also be noted that the hydrophilicity or the hydrophobicity of the membranes have a remarkable effect only at the initial stage of the fouling [97]. After the initial stage, the main influencing factor will be the chemical properties of the foulants on the surface. Improving the hydrophilicity of the membrane will result in improved permeability of the membrane due to the fouling reduction.

2.7.3. Membrane surface charge

Membrane surface charge is another membrane material property that affects the membrane fouling. If the membrane surface charge and the charge in the feed wastewater are opposite, it can increase the membrane fouling. Having same charge in membrane material and feed water can decrease the fouling due to the repellent effect of similar charges. Lee *et al.* [98] had utilized the graphene oxide (GO) in membranes to improve the antifouling property. They found that by increasing GO contents, the surface charge of the membrane surface, which is measured by Zeta potential, also increased. As most microbial products in aquatic system such as EPS have negatively charged surface, the high Zeta potential value of the membrane surface can induce electrostatic repulsive force with the microbial products to reduce the fouling on the surface.

2.7.4. Membrane surface roughness

The membrane surface roughness is an important physical property that would influence membrane fouling in MBRs. Rough surface has been found to increase the flux reduction apparently due to the reduced hydrodynamic shear in the proximity to the valley regions of the ridge-and-valley structure [99]. It has been found that membranes with homogeneous surface are less susceptible to be fouled than those with uneven surface [100]. Membranes with rough surface provides valleys for the accumulation of colloidal particles from the wastewater on the membrane surface, resulting in fouling by blocking the valleys [101]. It has been observed that higher projection on the outer surface showed a higher antifouling property. This can be explained by the observation that, after backwashing, the recovery of the permeability increased on the outer surface. The foulants were accumulated on the valley between the projections leaving the top of the projections clean [102]. Hence, rough surface may increase the fouling but rougher surface with protruding projections can trap their foulants in the valleys and still perform normally.

2.8 Technology gap

MBRs are extensively used in wastewater treatment process due to their lower space requirement and higher effluent quality than the conventional bioreactors; however, the major obstacle of MBR is membrane fouling, which negatively influence the membrane filtration performance by reducing the permeation flux. Modifying polymeric membranes by incorporating nanoparticles has been studied widely to mitigate the membrane fouling and to improve the property of the membranes. This modification of membrane surface alleviates the fouling by reducing the biofilm formation. Nevertheless, biofilm formation is in fact an important factor for organic removal from the wastewater to achieve a higher quality effluent. Considering these facts, this research is proposing an innovative hybrid membrane system where the membrane will satisfy different functionalities simultaneously by integrating macroporous open cell polymer foam with nanofibrous polymer membrane embedded with nanoparticles. The macroporous foam on the feed side will sustain the growth of biofilm to get higher organic removal efficiency and the nanoparticles embedded membrane on the permeate side will provide antimicrobial and antifouling property to the membrane surface.

Chapter Three: Effect of processing parameter of electrospinning on nanofibrous membrane

The aim of this study is to fabricate PVDF nanofibrous membrane via electrospinning process. The concentration of the PVDF solution used in this study was fixed at 20 wt.%. Different processing parameters of electrospinning such as applied voltage (i.e., 15 kV, 20 kV and 25 kV), flow rate of spinning solution (i.e., 0.5 mL/h, 1 mL/h, and 1.5 mL/h) and tip-to-collector distance (10 cm, 15 cm, and 20 cm) were used to fabricate PVDF nanofibrous membranes. Then, PVDF nanofibrous membrane with different loadings (i.e., 0 wt.%, 0.5 wt.%, 1 wt.%, and 1.5 wt.%) of MWCNT were prepared. Systematic analyses had been done to investigate the effects of the processing parameters of electrospinning and MWCNT loading on the morphology of the fabricated nanofibrous membranes.

3.1 Experimental

3.1.1 Materials

PVDF (Kynar 741, Arkema, with the molecular weight of $282\,000\text{ g}\cdot\text{mol}^{-1}$) was used without any further modification. The solvents used for electrospinning were DMF (ACS reagent, $\geq 99.8\%$) and acetone (ACS reagent $\geq 95.5\%$). 5 wt.% of multiwalled carbon nanotubes (MWCNT) in NMP solvent (ORGACYL™ NMP0502) were used as the source of nanoparticles during electrospinning.

3.1.2. Preparation of electrospun membrane

20 wt.% PVDF was dissolved in a solvent mixture of DMF and acetone with a DMF: acetone ratio of 7:3. The polymer solution was electrospun on an electronically grounded aluminum foil, applying high voltage through a high voltage power supply (0-30 kV, Model- ES30P-5W DDPM)

using the following procedures. For the fabrication of membranes loaded with MWCNT, 0.5 wt.%, 1 wt.% and 1.5 wt.% of MWCNT solutions was added to the 20 wt.% PVDF solution.

STEP 1. The polymer solution was stirred at 250 rpm and 50° C for 16 hours to achieve a homogeneous solution.

STEP 2. The polymer solution was loaded into a 10 mL syringe with a stainless-steel needle with 21 gauge for electrospinning.

STEP 3. The syringe was placed in a programmable syringe pump (Model LEGATO 100) to control the flow rate. The syringe tip was connected to a high voltage power supply.

STEP 4. The PVDF solution was electrospun for 3 hours on an electrically grounded aluminum foil with an applied voltage ranged from 15 to 25 kV at a flow rate 0.5 to 1.5 mL/h with tip to collector distance between 10 and 20 cm. For the case of PVDF-MWCNT solutions, the applied voltage, flow rate, and tip-to-collector distance were fixed at 20 kV, 1 mL/h and 15 cm, respectively.

STEP 5. The nanofibrous membrane were peeled from the foil paper after 24 hours to ensure the complete evaporation of the solvent.

3.1.3. Characterization

The morphological structures of the membranes were studied using scanning electron microscopy (SEM) (FEI Company Quanta 3D FEG). The samples were sputter-coated with platinum (Denton Vacuum, Desk V Sputter Coater). The average fiber diameter was measured from the SEM micrographs at 15000X magnification using the ImageJ software. For each electrospinning

condition, three samples were prepared, and 75 different fibers' diameters were measured from three different locations for each sample. The pore sizes of the electrospun membranes were measured using the ImageJ software.

The porosity of membrane can be defined as the volume of the pores present in the membrane divided by the total volume of the membrane. It can be determined using the following method [103]. After immersing the membranes into the isopropyl alcohol (IPA), which penetrates the pores of the membrane, the weight of the membrane with IPA was measured after removing the IPA from membrane surface. The porosity can be calculated by Equation (3.1).

$$\varepsilon_m = \frac{(\omega_1 - \omega_2) / D_i}{(\omega_1 - \omega_2) / D_i + \omega_2 / D_p} \quad (3.1)$$

where ω_1 is the mass of the wet membrane after immersing in the isopropyl alcohol (IPA), ω_2 is the mass of the dry membrane, g; D_i is the density of isopropyl alcohol, g/m³; D_p is the density of polymer, g/m³.

3.2. Results and discussion

3.2.1. Effect of flow rate on the morphology

In electrospinning process, the flow rate of the solution would affect the morphology the nanofibrous membrane. Figure 3.1 shows the morphology and the fiber diameter distributions of the samples fabricated with flow rate of 0.50 mL/h, 1.0 mL/h and 1.5 mL/h while keeping the applied voltage at 15 kV and a tip-to-collector distance of 15 cm.

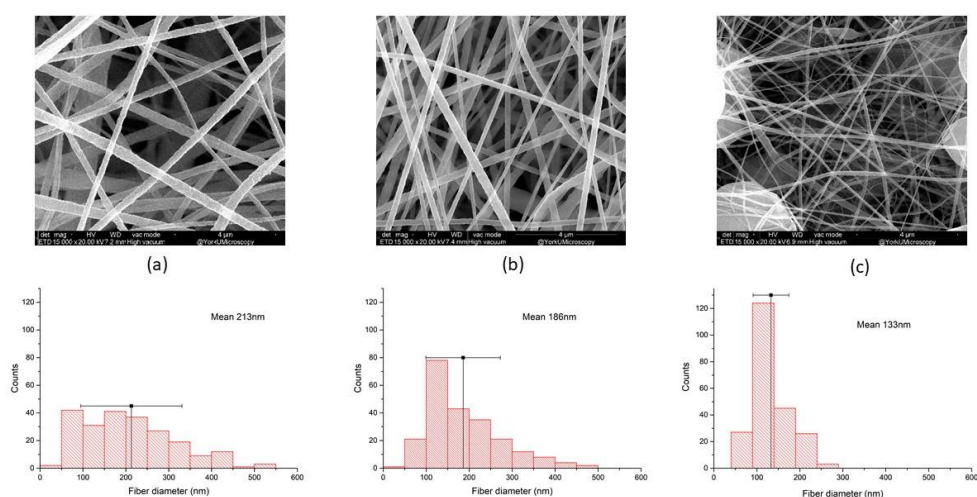


Figure 3. 1: Effect of flow rate on morphology and fiber diameter distribution (note: applied voltage = 15 kV, tip-to-collector distance = 15 cm) with flow rate of (a) 0.5 mL/h, (b) 1 mL/h and (c) 1.5 mL/hr. Magnification 15kX

It has been noticed that increasing the flow rate of the polymer solution reduced the average fiber diameter although the literature reported an opposite trend [104]. It is speculated that higher flow rate would reduce the time for the polymer solution to accumulate at the tip of the needle, leading to a decrease in fiber diameter. Furthermore, beads were observed in the electrospun fibers when the flow rate was 1.5 mL/h due to the unstable jet. The presence of beads may also be caused by insufficient drying time of the electrospun fibers when they reached the collector. As shown in Table 3.1, it is evident that changes in flow rate exhibited minimal effect on the average pore size.

At the lower flow rate of 0.5 mL/h, there is an increase in the variation of fiber diameter and the pore size. Variation in fiber diameter results in variation in pore size as overlapping of nanofibers form the nonwoven mesh. The one-way ANOVA (significance value $\alpha < 0.05$) test showed that there is no significance difference of mean pore size after changing the flow rate of the polymer solution as the p value from the test showed higher value than 0.05. However, the ANOVA test revealed that the mean porosity is significantly different and with 1.5 mL/h flow rate, the porosity was reduced to $80 \pm 3\%$ due to the presence of beads on the membrane. On the basis of this parametric study, an optimum flow rate of 1 mL/h was chosen to conduct the electrospinning processes in the investigation for other processing conditions as it gives the beadless fiber, higher porosity, uniformity of fiber diameter and pore size.

Table 3. 1: Effect of flow rate on fiber diameter, pore size and porosity. (Applied voltage= 15kV, tip to collector distance= 15cm)

Sample type	Flow rate (mL/h)	Fiber diameter (nm)	Pore size (nm)	Porosity (%)
(a)	0.5	213±100	218±186	87±5
(b)	1	186±57	244±31	89±2
(c)	1.5	133±3	218±15	80±3

3.2.2. Effect of applied voltage on the morphology

Figure 3.2 shows the effect of applied voltage on morphology and fiber diameter distribution. The experiments were carried out with the applied voltage of 15 kV, 20 kV and 25 kV, respectively, while keeping the flow rate at 1 mL/h and the tip-to-collector distance at 15 cm. The average fiber diameters, pore sizes, and porosities of electrospun samples prepared using different applied voltage are summarized in Table 3.2. It can be observed that increasing the applied voltage from 15 kV to 20 kV resulted in larger fiber diameter; however, the fiber diameter decreased when the applied voltage further increased to 25 kV. On the one hand, increasing the applied voltage would

increase the acceleration of the jet and reduce its flight time. Therefore, the fibers might not have enough time to be stretched and elongated before getting deposited [105], leading to an increase in fiber diameter. On the other hand, further increasing the applied voltage would also lead to higher electric field strength, which would increase the electrostatic repulsive force among the fibers formed from the solution increased, leading to thinner fibers. The one-way ANOVA (significance value $\alpha < 0.05$) test revealed that there is no significant difference in mean pore size and mean porosity of the membranes as the p value were higher in both cases.

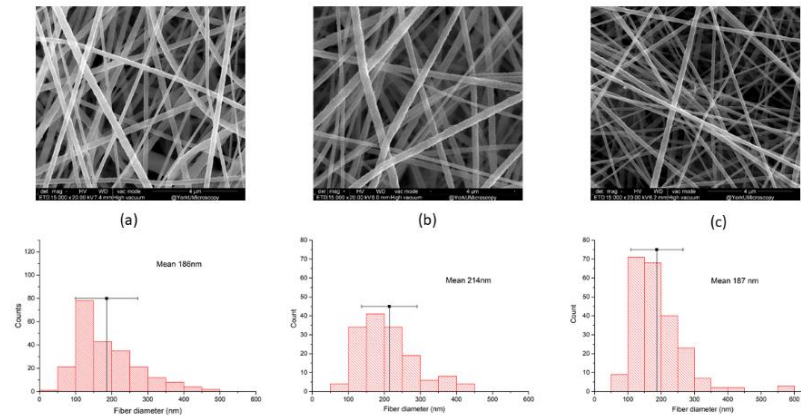


Figure 3. 2: Effect of applied voltage on morphology and fiber diameter distribution (flow rate=1mL/h, tip to collector distance= 15 cm) with applied voltage (a) 15 kV, (b) 20 kV and (c) 25 kV. Magnification 15 kX

Table 3.2: Effect of applied voltage on fiber diameter, pore size and porosity. (flow rate=1 mL/h, tip to collector distance= 15 cm)

Sample type	Applied voltage (kV)	Fiber diameter (nm)	Pore size (nm)	Porosity (%)
(a)	15	186±57	244±31	89±1
(b)	20	214±11	253±21	88±2
(c)	25	187±30	252±31	85±1

3.2.3. Effect of tip-to-collector distance on the morphology

It is important to have enough time for the solvent to evaporate from the polymer solution [104]. The time for the evaporation depends on the distance between the tip and the collector. In this set of experiments, electrospinning was conducted with different tip-to-collector distances, ranging from 10 cm to 20 cm while keeping the flow rate at 1 mL/h and the applied voltage at 15 kV. Table 3.3 shows that increasing the distance from 10 cm to 15 cm, the fibers diameter has been increased from 164 ± 20 nm to 186 ± 57 nm. It might be caused by the weakening of the electric field strength at longer tip-to-collector distance. Reduced electric field might affect the stretching of the polymer jet and resulted in thicker fiber diameter. However, fiber diameter decreases from 186 ± 57 nm to 181 ± 57 nm after increasing the tip-to-collector from 15 cm to 20 cm. The one-way ANOVA (significance value $\alpha < 0.05$) test showed that there is no significance difference of mean pore size after changing the tip to collector distance as the p value from the test showed higher value than 0.05. However, the one-way ANOVA test revealed that there is a significance difference in mean porosity and higher porosity of 89% was observed with 15 cm among other tip-to-collector distances.

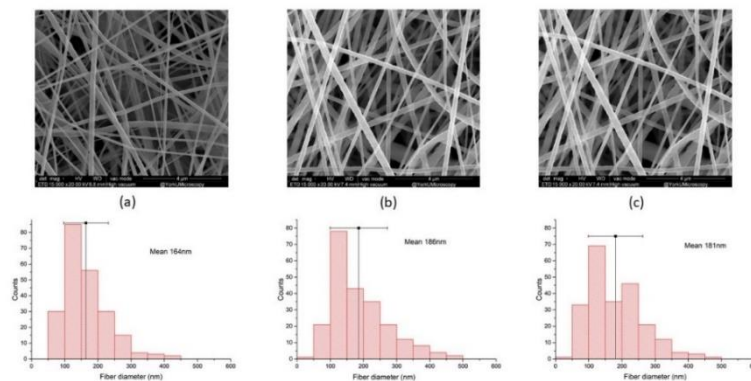


Figure 3. 3: Effect of tip to collector distance on morphology and fiber diameter distribution (applied voltage= 15kV, flow rate = 1mL/h) with tip to collector distance (a) 10cm, (b) 15cm and (c) 20cm. Magnification 15kx

Table 3.3: Effect of tip to collector distance on fiber diameter, pore size and porosity. (flow rate=1mL/h, applied voltage= 15kV)

Sample type	Tip to collector distance (cm)	Fiber diameter (nm)	Pore size (nm)	Porosity (%)
(a)	10	164±20	222±16	84±1
(b)	15	186±57	244±31	89±1
(c)	20	181±57	223±34	87±3

3.2.4 Effect of MWCNT contents on the morphology

Figure 3.4 shows the effect of MWCNT contents on morphology and fiber diameter distribution of the electrospun samples. Electrospinning was carried out by adding 0.5 wt.%, 1.0 wt.% and 1.5 wt.% MWCNT to the PVDF polymer solution with the flow rate, applied voltage, and tip-to-collector distance fixed at 1 mL/h, 20 kV and 15 cm, respectively. The fiber diameter decreased with the loading of MWCNT increased from 0.5 wt.% to 1 wt.%. Higher conductivity of the spinning solution with increasing amount of MWCNT, might be a reason for thinner fiber formation. Higher conductivity of the polymer jets results in an increase on the stretching of the polymer droplets, which decreases the fiber diameter [105]. Beads were formed with an increased amount of MWCNT (1.5 wt.%). It is believed that this could be due to increased viscosity of the solution and potential agglomeration of MWCNT during electrospinning [106]. The one-way ANOVA (significance value $\alpha < 0.05$) test showed that there is no significance difference of mean pore size and mean porosity after changing the MWCNT loadings as the p value from the test in both cases showed higher value than 0.05.

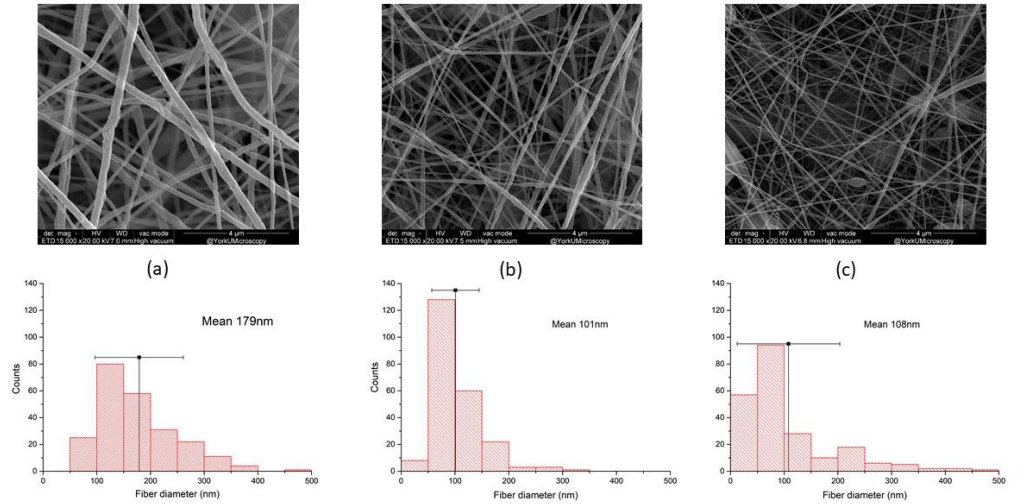


Figure 3. 4: Effect of MWCNT contents on morphology and fiber diameter distribution (flow rate = 1 mL/h, tip to collector distance = 15 cm, applied voltage = 20 kV) with MWCNT contents (a) 0.5wt.%, (b) 1wt.% and (c) 1.5wt.%. Magnification 15kx.

Table 3.4: Effect of MWCNT contents on fiber diameter, pore size and porosity. (flow rate=1mL/h, tip to collector distance= 15cm, applied voltage= 20kV)

Sample type	MWCNT (wt.%)	Fiber diameter (nm)	Pore size (nm)	Porosity (%)
(a)	0.5	179±35	260±75	83±4
(b)	1	101±25	256±65	84±2
(c)	1.5	108±85	260±77	84±1

3.3 Conclusion

This study investigated the effects of processing conditions such as flow rate, applied voltage, and tip-to-collector distance on the morphology of nanofibrous membrane prepared by the electrospinning process. Current investigation shows that the fiber diameter is decreased when the flow rates increased, and beads are formed when the solution flow rate is increased to 1.5 mL/h

due to the unstable jet or by insufficient drying time of the electrospun fibers when they reached the collector. The ANOVA test showed that the flow rate had minimal effect on the pore size of the membranes. With 1.5 mL/h flow rate, the porosity was reduced to $80 \pm 3\%$ due to the presence of beads on the membrane. The membrane exhibits the highest porosity (i.e., $89 \pm 2\%$) with 1 mL/h flow rate. The effect of increasing applied voltage shows two different trends in the change of fiber diameter. However, the applied voltage had no significant effect on the pore size and porosity of the membranes. The fiber diameter increases when the tip-to-collector distance increases from 10 cm to 15 cm due to the weakening of the electric field strength and then the fiber diameter decreased when the tip-to-collector distance increases from 15 cm to 20 cm. There was no major change in pore size after increasing the tip-to-collector distance. Membranes prepared with 15 cm tip-to-collector showed the porosity of $89 \pm 2\%$. Considering all the findings from the effect of processing parameters on electrospinning, the combination of 20 kV applied voltage, 1 mL/h flow rate and 15 cm tip to collector distance had been used to prepare the PVDF/MWCNT electrospun membranes, as this condition gave the bead-less nanofibers with higher porosity among all the other conditions. The fiber diameter decreased with the loading of MWCNT increased from 0.5 wt.% to 1 wt.% due to the higher conductivity of the spinning solution with increasing amount of MWCNT. Moreover, SEM micrographs of the nanofibers showed the presence of beads with the addition 1.5 wt.% of MWCNT in the PVDF spinning solution due to the agglomeration of nanoparticles with high concentration of MWCNT. The ANOVA test revealed the MWCNT loadings had minimal effect on the pore size and the porosity of the membrane. In later chapter this PVDF/MWCNT nanofibrous membranes will be integrated with open-cell polymer foams to fabricate a multifunctional membrane structure.

Chapter Four: Multifunctional membrane system in wastewater treatment

The aim of this chapter is to design and develop a multifunctional polymer-based nanofibrous membrane system that integrates a nano or micro-porous membrane and a porous biofilm carrier for a biological wastewater treatment system. The active surface of the membrane will be a macro-porous open-cell foam, which will sustain the growth and the activity of biofilm for enhanced organic removal. The unique characteristics of open-cell foam such as a high level of interconnectivity among their cells, high porosity and high surface roughness make them a potential habitat for the microbial immobilization as a biofilm carrier [107]. And the nanofibrous membrane embedded with MWCNT will provide antimicrobial and antifouling effect to reduce the fouling. In the previous chapter (Chapter 3), PVDF nanofibrous membranes were prepared with 0.0 wt.%, 0.50 wt.%, 1.0 wt.% and 1.5 wt.% MWCNT via electrospinning process using 20 kV applied voltage, 15 cm tip to collector distance and 1 mL/h flow rate. In this chapter, the effect of MWCNT contents on the multifunctional membrane morphology, filtration performance and the organic removal efficiency of the membranes will be investigated. For this purpose, PVDF open-cell foam with 80 wt.% leaching agents (i.e., NaCl) with particle sizes less than 250 μm was manufactured. Then, the open-cell foam was attached to the PVDF nanofibrous membranes containing (0 wt.%, 0.50 wt.%, 1.0 wt.% and 1.5 wt.% MWCNT) by supercritical CO₂ foaming process.

4.1 Experimental

4.1.1. Materials

PVDF (Kynar 741, Arkema, with the molecular weight of 282 000 g·mol⁻¹) was used without any further modification. Sodium chloride (NaCl, Windsor) was used as leaching agent to produce open-cell structures. Carbon dioxide (CO₂, purity 99.8%, Linde Gas Inc.) was used as the physical foaming agent and was pumped to a high-pressure high temperature chamber.

4.1.2. Preparation of open-cell foam

PVDF powders were blended with sieved NaCl particles less than 250µm in particle size. The polymer-salt mixture loaded with 80 wt.% of leaching agents was molded by a compression molding machine (Craver Press, 4836 CH) into cylindrical samples (i.e., the diameter and height of each sample were 20mm and 2mm, respectively) by the following steps:

STEP 1. PVDF-leaching agent mixtures were loaded into mold and subsequently transferred into the compression molding machine with a pre-set temperature of 185°C.

STEP 2. The mold was maintained in contact with the top and bottom heating platens for 5 minutes without increasing the pressure to completely melt the PVDF.

STEP 3. The samples and mold were pressurized to 5000 lbs-force for 5 minutes, and subsequently to 10 000 lbs-force for 10 minutes.

STEP 4. The mold was removed from the compression molding machine and was loaded into a cooling module with circulating water for 10 minutes to cool down the molded samples.

STEP 5. Each sample was immersed in 500 mL of deionized water for 72 hours to leach out NaCl from the PVDF matrix. Deionized water was replaced every 24 hours to avoid saturation of salt.

STEP 6. Samples were dried in an oven at 60°C for 24 hours.

4.1.4. Preparation of multifunctional membrane structure

PVDF open-cell foam and PVDF electrospun nanofibrous membranes with different MWCNT loadings prepared as described in the previous chapter were cut into circular pieces (diameter 20mm) and enclosed into a high-pressure high temperature chamber. The chamber was then heated up to the saturation temperature (i.e., 130 °C). Once the chamber had reached the saturation temperature, CO₂ was injected into the chamber at 1500 psi for 15 minutes using a syringe pump. After saturating the sample with supercritical CO₂ for 15 minutes, the gas was released by opening the outlet valve. Finally, the sample was taken out and submerged into an ice bath to stabilize the structure.

4.1.5. Experimental setup and operation

Dead end filtration cells of 250 mL were used to set up the membrane bioreactor. The effective volume of the membrane bioreactor was 250mL. Air was supplied to the membrane bioreactor using an air pump with bubble diffuser to supply oxygen for microorganisms in the membrane bioreactor and to promote the uniform distribution of dissolved oxygen. The filtration cell was placed on the orbital shaker at 100 rpm to avoid concentration polarization of the seed water. Vacuum pump was connected with each cell for the filtration. Each bioreactor was filled with 100 mL of activated sludge with MLSS concentration of 550 mg/L and 100 mL of synthetic wastewater with sCOD value of 250 mg/L. The used activated sludge in this study was collected from Humber Wastewater Treatment Plant and then nourished with synthetic wastewater for 2 days to activate the microorganism. During the test, the activated sludge has been fed with 50 mL of synthetic wastewater each day as a feed to the microorganisms. The compositions of the synthetic wastewater are given below in Table 4.1.

Table 4. 1: Composition of synthetic wastewater

Components	Amount (mg/l)
<i>Chemical Compounds</i>	
Urea	1600
NH ₄ Cl	200
Na-acetate.3H ₂ O	2250
Peptone	300
MgHPO ₄ .3H ₂ O	500
K ₂ HPO ₄ .3H ₂ O	400
FeSO ₄ .7H ₂ O	100
CaCl ₂	100
<i>Food Ingredients</i>	
Starch	2100
Milk powder	2100
Dried yeast	900
<i>Trace Metals</i>	
Cr(NO ₃) ₃ .9H ₂ O	15
CuCl ₂ .2H ₂ O	10
MnSO ₄ .H ₂ O	2
NiSO ₄ .6H ₂ O	5
PbCl ₂	2
ZnCl ₂	5

A schematic of filtration set up has been shown in Figure 4.1.

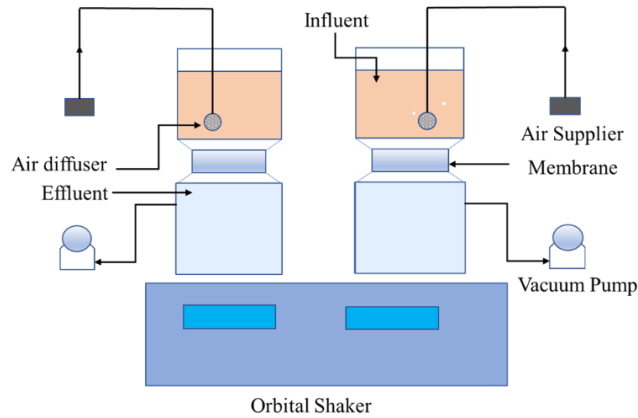


Figure 4. 1: Filtration Set up

The synthetic wastewater was diluted with water to get the sCOD value of 250 mg/L. The sCOD in the suspended liquid phase was measured to evaluate the amount of soluble organic matters contributed by the added substrate. To measure the sCOD measurement, collected water samples were filtered by a syringe filter with an average pore size of 0.45 μm to eliminate solid particles from the solution. The 2 mL filtered samples were then injected into COD vials and loaded into the digester for 2 hours at 150 $^{\circ}\text{C}$. After digestion of the samples in the COD vials, the samples were cooled to room temperature and sCOD was determined by COD analyzer (HACH, DR 3900). Total suspended solid (TSS) of the water samples were measured. In order to measure the amounts of TSS, a known volume (v) of the sample was injected into a pre-weighed glass microfibre filter with 1.2 μm particle retention and loaded onto an aluminium pan. The total mass of the dried sample, filter, and pan is denoted as m_1 . They were then dried in an oven at a temperature of 105 $^{\circ}\text{C}$ for 2 hours. Equations were used to determine the TSS of the collected water samples.

$$\text{TSS} = \frac{m_2 - m_1}{V} \quad (4.1)$$

4.1.6 Characterization

SEM (FEI Company, Quanta 3D FEG) was used to characterize the multifunctional membrane's structure and the biofilm structure. To prepare the cross-section of the membranes the samples were cryo-fractured under liquid nitrogen and the fractured surfaces then sputter coated with platinum (Denton Vacuum, Desk V Sputter Coater). To observe the surface of the open-cell foam and the nanofibrous surface of the membranes, both were sputter coated with platinum. After biological process, to analyze the biofilm the membranes have been cut with sharp blade to observe the cross-section of the membranes.

Contact angle of the membranes was measured by using contact angle analysis instrument (KRUSS FM40 EASY DROP). 3 μ L of deionized was placed on the membrane surface and the angle between the membrane and water surface was recorded. The measurement was reported from 5 different locations of the membranes.

Pure water flux was measured using a dead-end cell containing 250 mL distilled water. The effective surface area of the membrane was 1.2 cm² and the applied vacuum pressure was 90 kPa. The water flux was measured using the following Equation (4.2).

$$\text{Flux } (J_{w1}) = \frac{V}{A t} \quad (4.2)$$

where V is the volume of permeate (L), A is the effective area (m²) of the electrospun membrane and t is the time (h) of water permeation.

The fouling resistance ability of the membrane can be determined by measuring the flux of activated sludge. For the purpose of activated sludge filtration, after the pure water flux measurement, the distilled water in filtration cell is replaced by activated sludge and the activated sludge flux of membrane J_s (L/m²h) can be measured. Afterward, the fouled membrane put in a conical-bottom centrifuge tube which was filler with 50 mL deionized water. Then the tubes were put in the sonicator device (VWR company, symphony™) to clean the membrane. The process was run for 20 minutes at 40°C and the pure water flux of cleaned membranes were measured anew as J_{w2} (L/m²h). To analyze the fouling property of prepared membranes, the flux recovery ratio (FRR) can be calculated by following Equation (4.3). It should be noted that the higher FRR shows the superior antifouling property of membranes.

$$FRR = \left(\frac{J_{w2}}{J_{w1}} \times 100 \right) \quad (4.3)$$

where J_{w1} is pure water flux and J_{w2} is pure water flux after cleaning the membrane.

Membrane retention efficiency which is also known as rejection can be calculated by following Equation (4.4).

$$R = (1 - C_p/C_f) \times 100 \quad (4.4)$$

where R is the rejection (%), C_f is the TSS of the feed (mg/L), and C_p is the TSS of the permeate (mg/L).

sCOD of the seed and permeate from the membrane bioreactor was measured by COD analyzer (HACH, DR 3900) as a representation of the soluble organic materials in the water. Then sCOD removal efficiency has been calculated from the following Equation (4.5)

$$\text{sCOD removal efficiency} = \left(\frac{\text{sCOD of seed}}{\text{sCOD of permeate}} \times 100 \right) \quad (4.5)$$

4.2 Results

4.2.1 *The morphology of the multifunctional membranes*

In this study, supercritical CO₂ processing has been used to improve the adhesion of the electrospun nanofibrous membrane to the polymer foam. The solvent (i.e., supercritical CO₂) penetrated the polymer and it facilitate the mobility of the chains, allowing the reorientation of the chain to form more thermodynamically favorable crystalline state [108]. Figure 4.2 shows the morphology of the multifunctional membrane before and after the supercritical CO₂ processing. The open-cell foam prepared by the salt leaching method has pore size less than 250µm. After supercritical CO₂ processing, it can be observed that more visible pores existed on the surface of the open-cell foam.

The supercritical CO₂ processing has been carried out at 130⁰C, which is below the melting point of PVDF, to attach the open-cell foam and the electrospun fiber together without damaging their structures. After the supercritical CO₂ processing, the electrospun nanofibrous membranes became compact and some overlapping of nanofiber was observed. The overlapping of fibers tends to fuse fibers together due to heat and is expected to have improved integrity and mechanical strength [109].

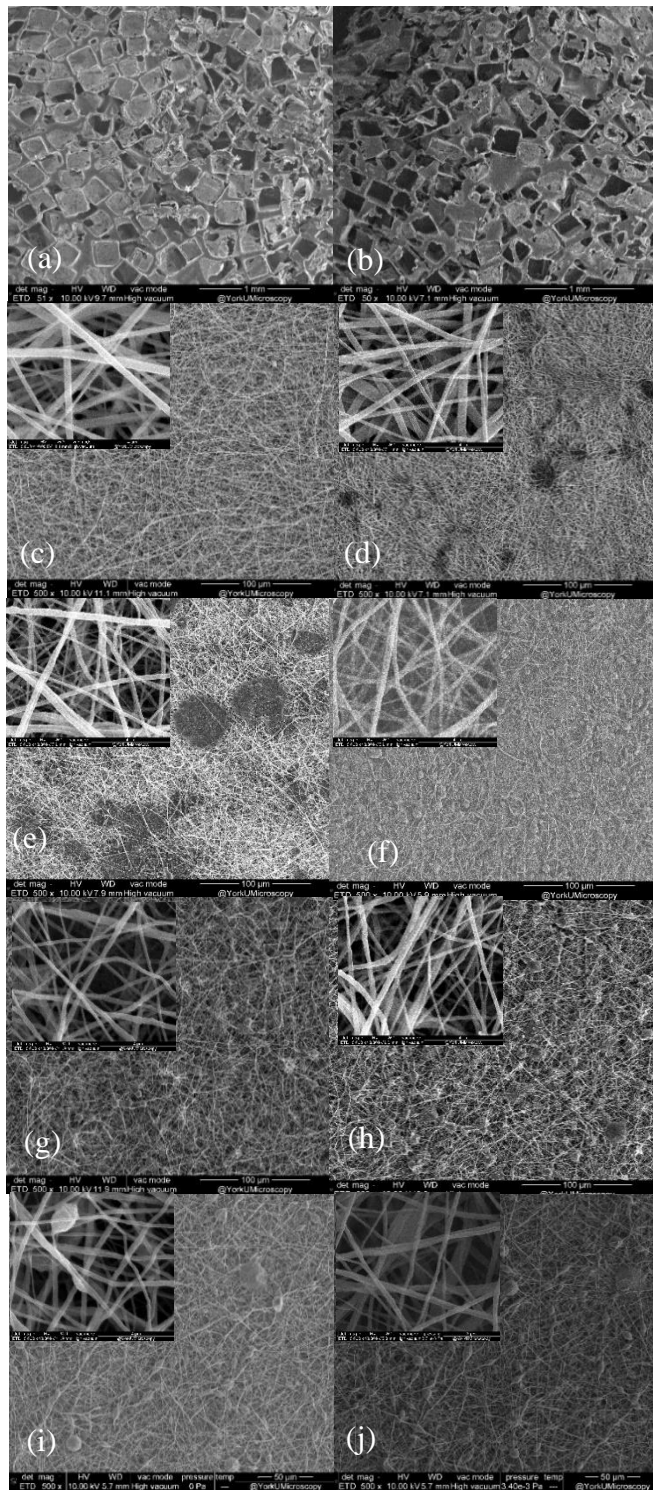


Figure 4. 2: SEM micrograph of multifunctional membranes at 50X (a) open-cell foam (b) open-cell foam after ScCO₂ and electrospun nanofiber at 500X with (c) 0 wt.%, (d) 0% MWCNT after ScCO₂, (e) 0.5 wt.%, (f) 0.5 wt.% MWCNT after ScCO₂, (g) 1 wt.% (h) 1 wt.% MWCNT after ScCO₂, (i) 1.5 wt.% and (j) 1.5 wt.% MWCNT after ScCO₂

Figure 4. 2 shows the SEM micrographs of the cross-section of the multilayer structures (i.e., open cell foam and nanofibrous membranes) attached together. According to the SEM micrographs, the thickness of the nanofibrous layer is different for membranes with different amounts of MWCNT loadings. The thickness of the nanofibrous layer of the membranes has been measured with three different samples to get a clear idea of the thickness of the membranes. Figure 4.3 is showing the thickness of the membranes.

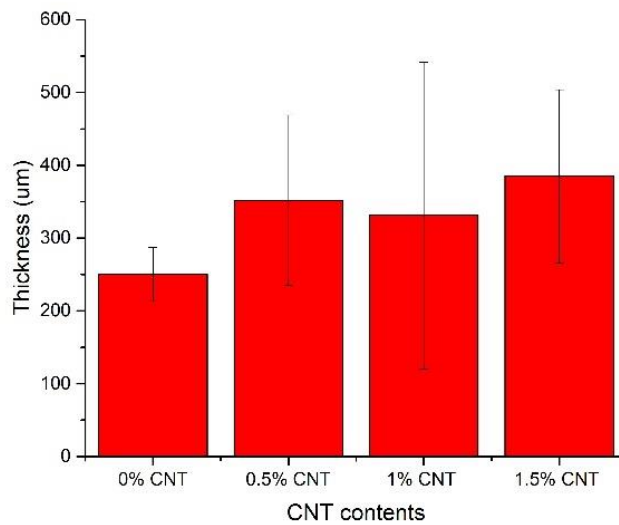


Figure 4.3: Thickness of the nanofibrous membrane

The thickness of the nanofibrous membrane was measured from the SEM micrographs of the cross-section of the membrane. The one-way ANOVA (significance value $\alpha < 0.05$) test had been conducted to analyse the statistical difference of the membrane thickness. The test revealed that the thickness of the nanofibrous membrane were statistically different as the p value in the test was 0.000158 which rejected the null hypothesis. And the thickness of the membranes with

MWCNT loading was higher than pristine PVDF membranes. This might be due to the presence of beads in the membranes which contributed to the increased thickness.

The SEM micrographs of the cross-section of the multilayer in Figure 4.4 (i.e., a and d) and Figure 4.5 (i.e., a and d), show the attachment between the open-cell foam and the nanofibrous membranes. Figure 4.4 (i.e., b and e) and 4.5 (i.e., b and e) shows the cross section of open-cell foam with interconnected cubic shape pores. The SEM micrographs of the cross-section of the nanofibrous membranes in Figure 4.4 (i.e., c and f) and Figure 4.5 (i.e., c and f), show the presence of beads with 1 wt.% and 1.5 wt.% MWCNT/PVDF membranes. With the higher amount of MWCNT loadings, the presence of beads increases. The formation of the beads was due to the agglomeration of the MWCNT particles in polymer spinning solution.

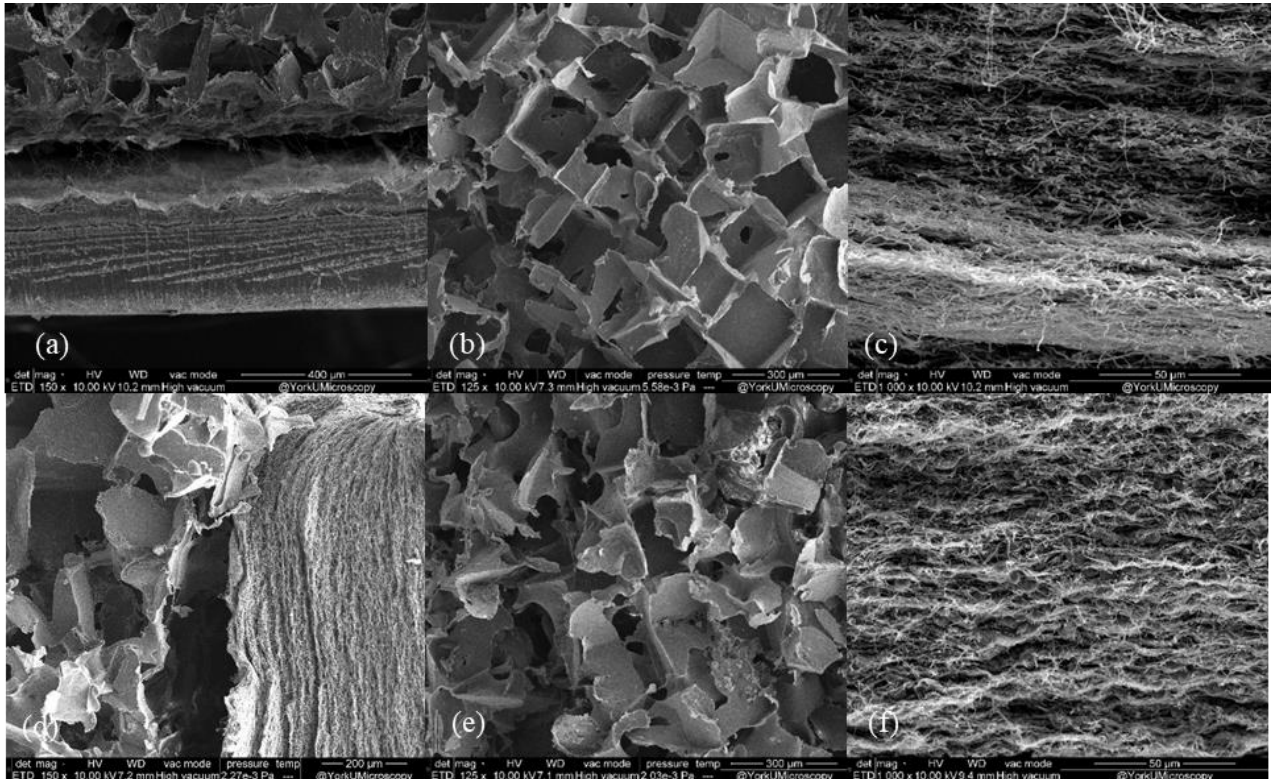


Figure 4. 4: SEM micrograph of the cross-section of membranes with 1% MWCNT (a) multilayer, (b) open-cell foam, (c) nanofibrous membrane; with 1.5% MWCNT (d) multilayer, (e) open-cell foam, (f) nanofibrous membrane.

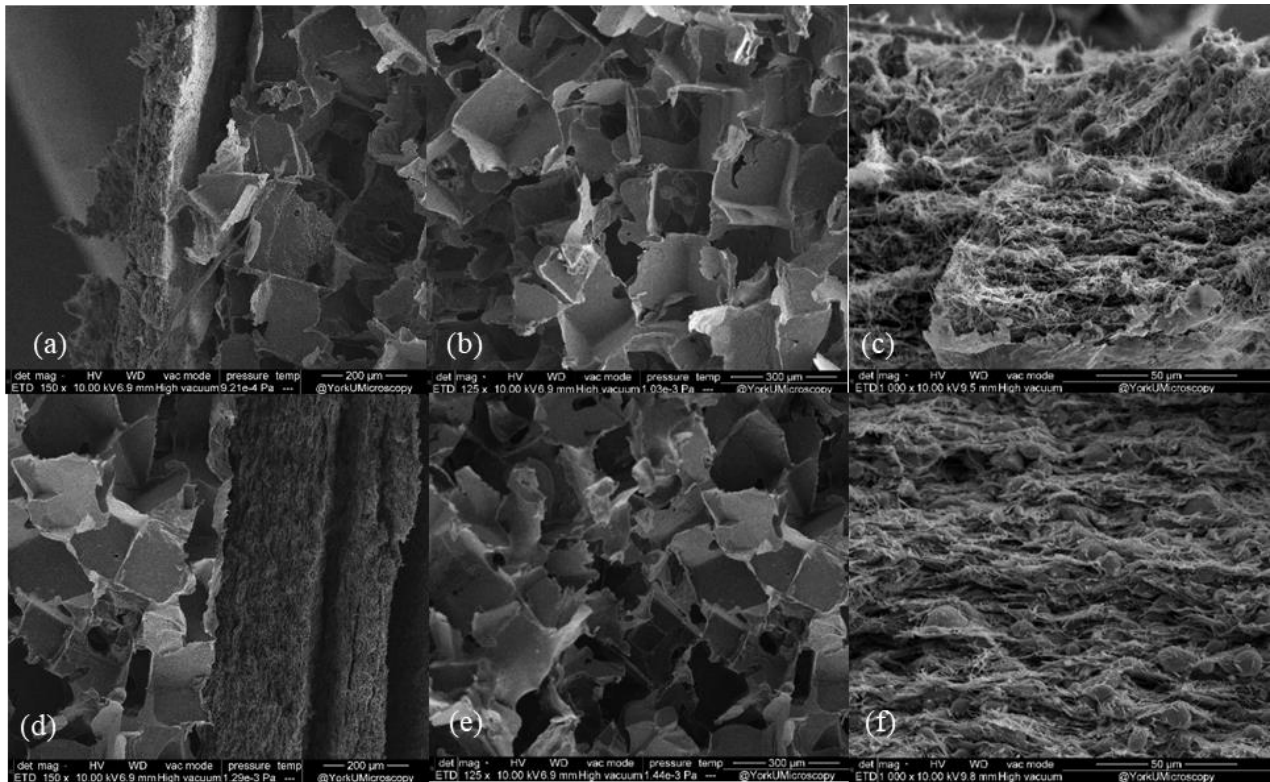


Figure 4.5: SEM micrograph of the cross-section of membranes with 0% MWCNT (a) multilayer, (b) open-cell foam, (c) nanofibrous membrane; with 0.5% MWCNT (d) multilayer, (e) open-cell foam, (f) nanofibrous membrane.

Figure 4.6 is showing the prepared multifunctional membrane system before using them for filtration, where nanofibrous membranes are integrated with open-cell foam.

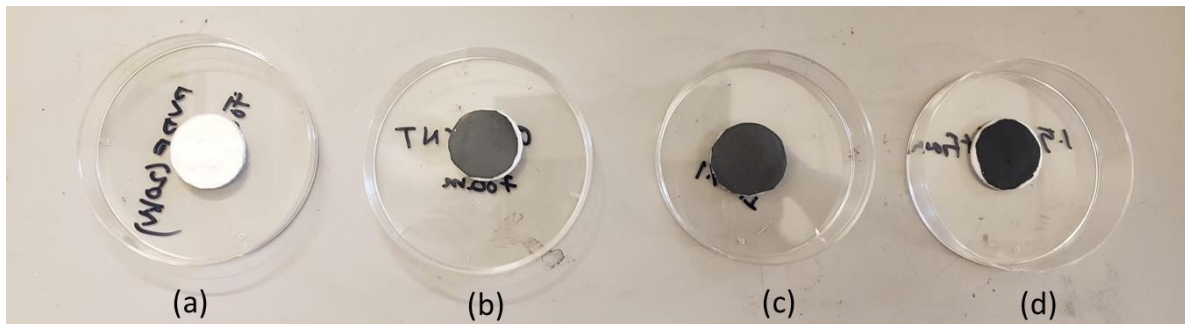


Figure 4.6: Multifunctional Membranes with (a) 0 wt%, (b) 0.5 wt%, (c) 1wt% and (d) 1.5 wt% MWCNT.

4.2.2. The effect of MWCNT contents on the contact angle of multifunctional membranes

The contact angle between the pure water and the multifunctional membrane is one of the ways to characterize the hydrophilicity of the membrane surface. When water is applied to the surface, the outermost surface layer interacts with the water. A hydrophobic surface with low free energy gives a high contact angle with water, whereas a wet high-energy surface allows the drop to spread by giving a lower contact angle.

Figure 4.7 shows the water contact angle of the membrane surface at different concentrations of MWCNT (i.e., 0 wt.%, 0.5 wt.%, 1 wt.%, 1.5 wt.%). The experimental result indicates that contact angle decreased with the addition of MWCNT. For the PVDF membrane the contact angle is 124 degrees. As shown in the diagram increasing the MWCNT concentration, the contact angle reached to 84 degrees. The addition of MWCNT nanoparticles made the membrane surface more hydrophilic, which was desirable to achieve antifouling property of the membranes.

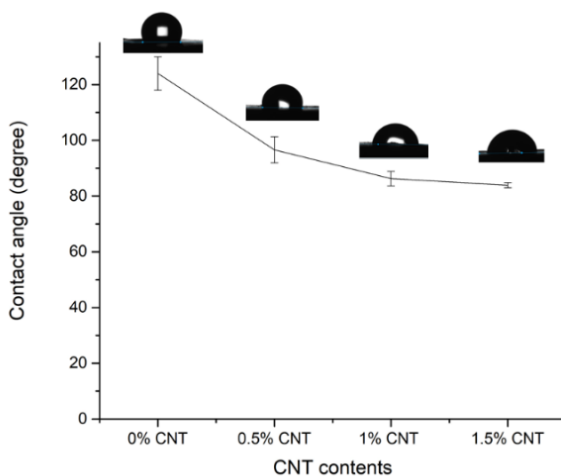


Figure 4.7: Water contact angle of membranes with 0 wt.%, 0.5wt.%, 1 wt.% and 1.5wt.% MWCNT

4.2.3. The Effect of MWCNT contents on permeation flux

Membrane hydrophilicity is one of the most important parameters that affects the permeation flux of the membranes. The pure water flux of the multifunctional membranes has been presented in Figure 4.8 (a) in which membranes with 1.5 wt.% MWCNT shows the highest pure water flux of 338 L/m²h among the other membranes. The pure water flux increased from 145 L/m²h in pristine PVDF membrane to 172 L/m²h after incorporation of 0.5 wt.% MWCNT in the PVDF solution for electrospinning. For 0.5 wt.%, 1 wt.% and 1.5 wt.% MWCNT, respectively, the pure water flux increased after increasing the MWCNT in the PVDF spinning solution. The pure water flux had been improved to two times after the addition of 1.5 wt.% MWCNT in the PVDF polymer solution.

Again, the flux of the multifunctional membranes had been measured with the synthetic wastewater with sCOD value of 250mg/L and tCOD value of 1000mg/L. Figure 4.8 (b) shows the measured flux for synthetic wastewater. The water flux with 1.5 wt.% MWCNT membrane was two times higher than the flux of pristine PVDF membrane. The water flux of synthetic wastewater was lower than the pure water flux for all the prepared membranes because of the presence of particulates in the wastewater, which was affecting the permeability of the membranes by blocking the pores of membranes.

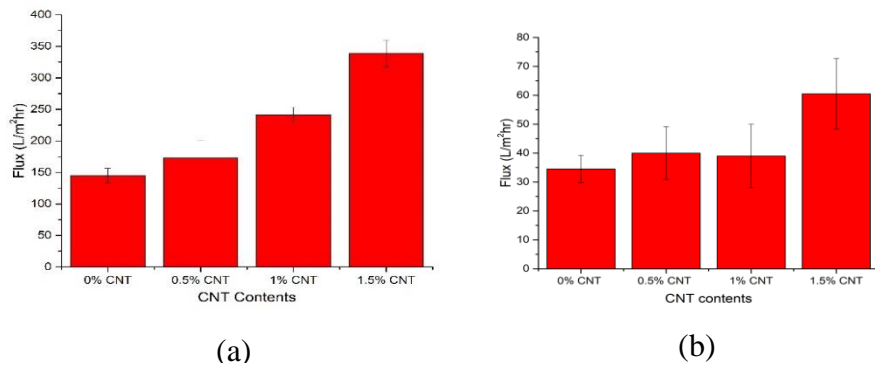


Figure 4.8: Effect of MWCNT loadings on (a) pure water flux and (b) synthetic wastewater flux of multifunctional membranes

4.2.4. Evaluation of multifunctional membranes performance with activated sludge

The filtration performance of multifunctional membranes had been evaluated in filtration cell with activated sludge in order to assess the flux and the biofilm formation on the membrane. The electrospun membrane with the biofilm carrier was built to provide a higher surface area for the biofilm formation which will improve the organic removal efficiency of the bioreactors. The active surface of the multifunctional membrane system is a macro porous open-cell foam was for the growth and activity of the biofilm to produce high grade effluent. The open-cell foam was the seed side of the membrane which is the active surface for the filtration and the nanofibrous membranes is on the permeation side to provide the antibacterial property and the micro pores were for particles rejection during the filtration test. To conduct the filtration of the activated sludge, the dead-end filtration cell was filled with 100 mL of activated sludge and 100 mL of synthetic wastewater. The filtration test with activated sludge was performed for 2 days and each day the activated sludge was fed with 50mL of synthetic wastewater to provide the food for the microorganisms. Figure 4.9 shows the flux of the membranes after 2 days. The activated sludge flux value of the membranes for 2 days experiment shows that 0.5 wt.% MWCNT membranes had higher flux than other membranes containing different amounts of MWCNT loading. The variable thickness of the nanofibrous membranes might affect the flux of the membranes.

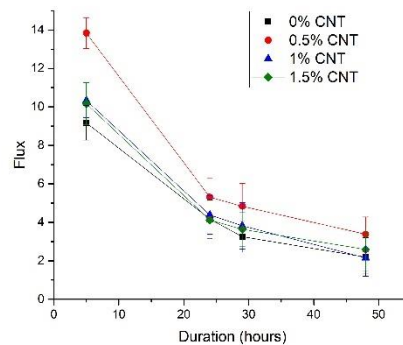


Figure 4.9: Effect of MWCNT loading on activated sludge flux for two days filtration test.

Then the filtration test conducted for 5 days, and the flux of the membranes had been measured each day after 5 hours and 24 hours, The results are shown in Figure 4.10 (a). The one way ANOVA (significance value $\alpha < 0.05$) test had been conducted to analyze the statistical difference of the activated sludge flux with different loadings of MWCNT. The test revealed that for each day the activated sludge flux of the membrane for different loadings of MWCNT were not statistically different as the p value from the test showed higher value than 0.05, and the graphs was not showing any definite trend of flux with different loading of MWCNT. This may be due to the different thickness of the membrane, or the experimental error caused by collecting the effluent each day. So, to avoid this we did the filtration test for 10 days and collected the effluent after each 5 days to measure the flux.

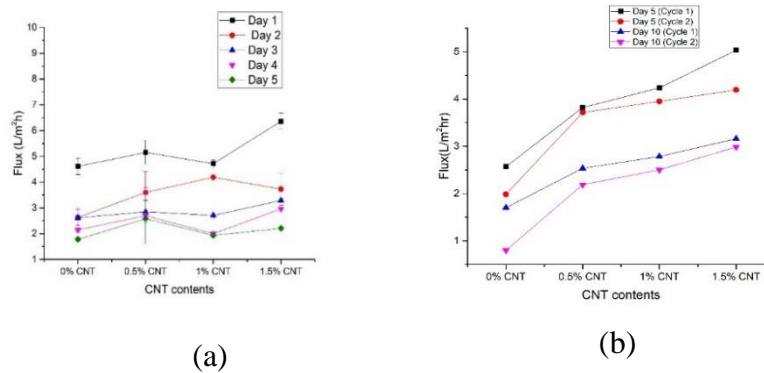


Figure 4. 10: Effect of MWCNT loading on activated sludge flux for (a) 5 days and (b)10 days filtration test

The Filtration tests had been conducted for 10 days with activated sludge in 2 cycles. In cycle 1, the flux had been measured after every 5 days to evaluate the filtration performance of the membranes. Then after 10 days, the membranes had been cleaned for 20 minutes at 40⁰C in the sonicator and they were being used for filtration test for 10 days in cycle 2. Figure 4.10 (b) shows the flux of the membranes for cycle 1 and cycle 2. The flux increased with an increasing amount

of MWCNT in the polymer solution of the membranes. The experimental results showed that the flux in cycle 2 was not significantly different from that in cycle 1, which indicated the reusability of the membranes. The experimental results indicate that on day 5, the flux increased with an increasing amount of MWCNT loadings due to the improved hydrophilic property of the membranes. However, with an increasing amount of time on 10 days, the flux was less likely to increase with an increasing amount of MWCNT loadings. The reason is that, with the increasing amount of filtration time, fouling not only depended on the hydrophilicity of the membrane also on the chemical property of the foulants.

4.2.5. Antifouling property and organic removal efficiency of the multifunctional membrane

The fouling resistance of the membranes was evaluated by measuring the pure water flux of the fouled membranes after 10 days of filtration with activated sludge. Figure 4.11 shows the calculated FRR value, which indicated the measure of the fouling resistance nature of the membrane. Pristine PVDF membranes show 40% of FRR whereas membranes with MWCNT show FRR value of 60%. This indicates the presence of nanoparticles improved both the antifouling property and the reusability of the membranes.

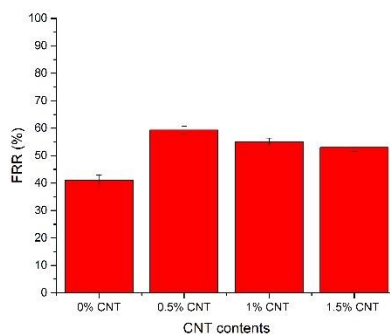


Figure 4.11: Effect of MWCNT loadings on the FRR of multifunctional membranes.

The membrane retention efficiencies for 5 days and 10 days have been shown in Figure 4.12 and the values indicate that after 5 days and 10 days the rejection was above 90% for all the membranes. Though the membranes with different MWCNT loadings show different flux values in the previous experimental results, the membrane retention efficiency was almost similar for all the membranes. Therefore, it can be concluded that fouling in the membranes did not have any effect on membrane retention efficiency.

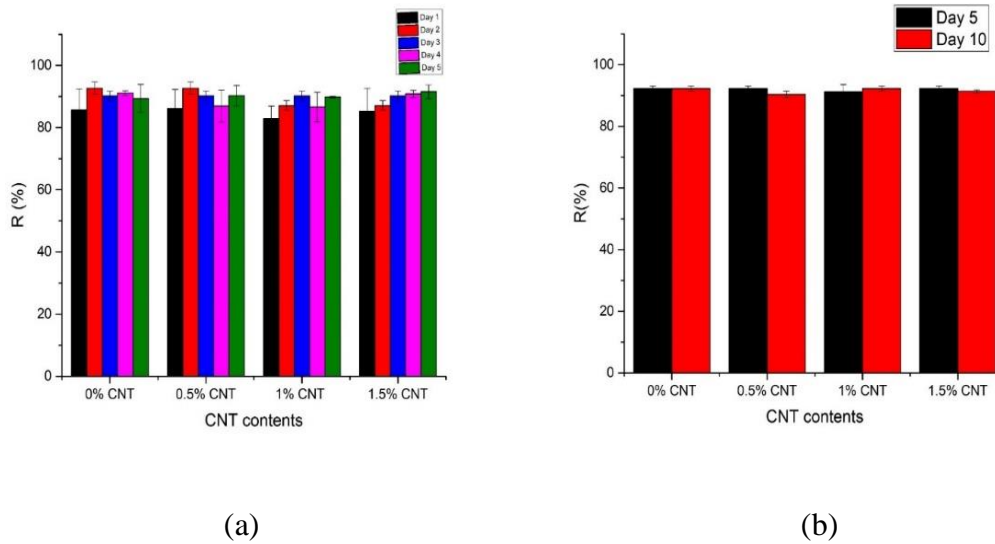


Figure 4.12: Effect of MWCNT loadings on the membrane retention efficiency of multifunctional membranes for (a) 5 days and (b) 10 days filtration test.

To evaluate the effect of biofilm carrier with the membranes for organic removal in the bioreactor, sCOD changes were investigated. Figure 4.13 (a) shows the sCOD removal efficiency of the bioreactor for 5 days experiment and the graph shows the sCOD removal efficiency for each day. From the results it is observed that for all the membranes started to increase with time and after day 5, the value reached to around 85%. Figure 4.13 (b) shows the sCOD removal efficiency of the bioreactor for 10 days experiment and the graph shows the sCOD removal efficiency for after 5 days and 10 days. The sCOD removal efficiency increased after 10 days experiments. It is

also evident that all the membranes showed the similar values of sCOD removal efficiency as all the membrane structure had similar open cell foam structure as biofilm carrier. Though the membrane structure had different loadings of CNT in the membranes, it did not affect the organic removal efficiency of the bioreactor. The formation of biofilms on the open cell foam and nanofibrous membranes was shown later in this chapter.

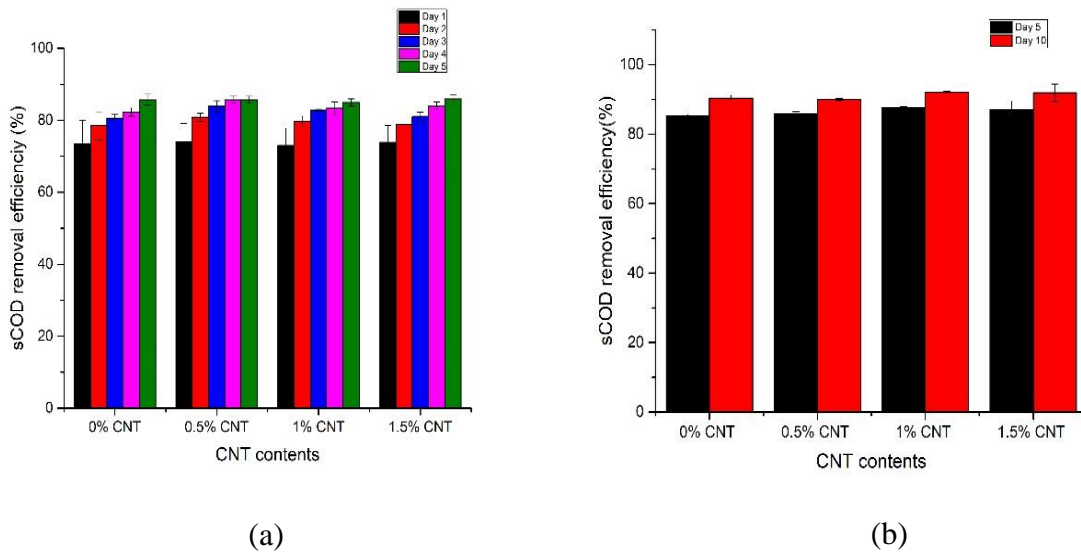


Figure 4.13: Effect of MWCNT loadings on the sCOD removal efficiency of multifunctional membranes for (a) 5 days and (b) 10 days filtration test.

The Figure 4.14 (a-d) shows the multifunctional membrane systems after being used for activated sludge filtration for 10 days. Figure 4.14 (e-h) shows the seed side of the membrane which is the microporous biofilm carrier and Figure 4.14 (i-l) shows the permeate side of the membrane of cleaned membranes after the sonication for 20 minutes.

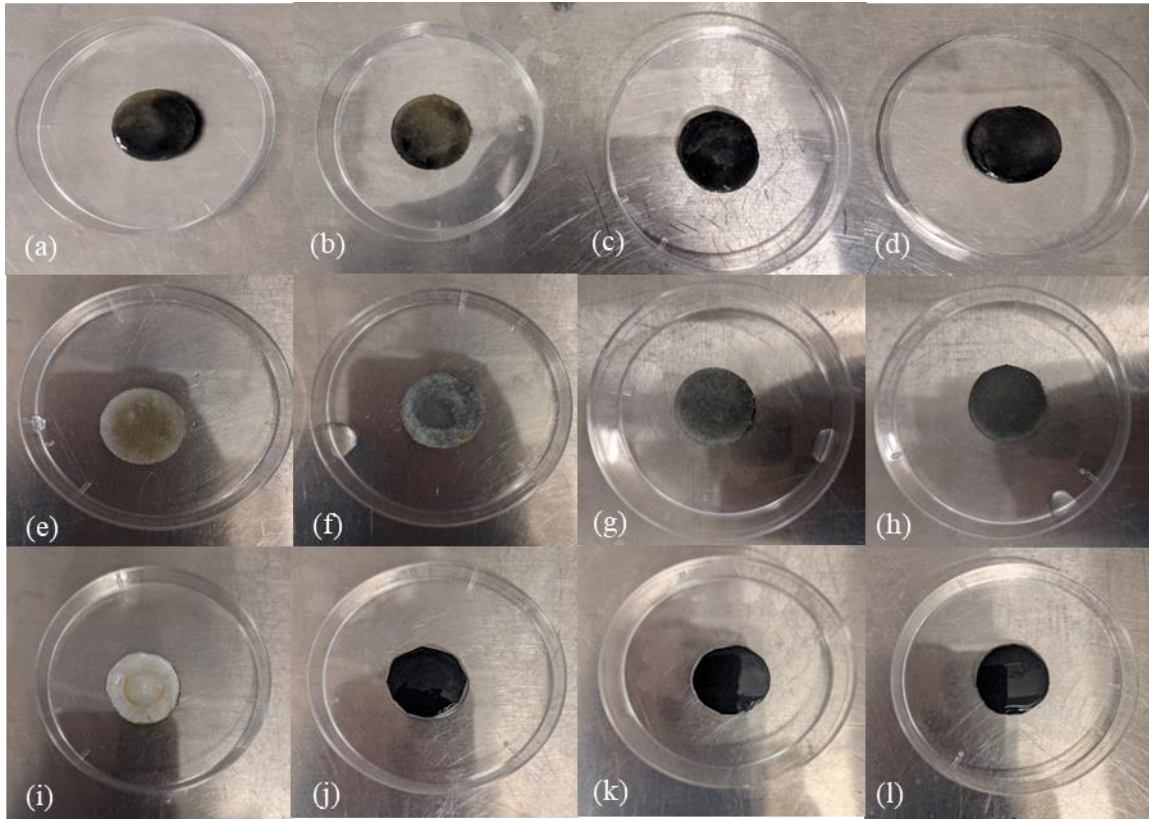


Figure 4.14: Multifunctional membrane after filtration with activated sludge with MWCNT loadings (a) 0 wt.%, (b)0.5 wt.% (c)1 wt.%, (d) 1.5wt.%; after cleaning the membrane the feed side with MWCNT(e) 0 wt.%, (f)0.5 wt.% (g)1 wt.%, (h) 1.5wt.%; and the permeate side with MWCNT(i) 0 wt.%, (j)0.5 wt.% (k)1 wt.%, (l) 1.5wt.%

Figure 4.15 shows the SEM micrographs of the feed side of the multifunctional membrane system with biofilm carrier after 10 days filtration test with activated sludge. The SEM micrographs of the macroporous biofilm carrier show the formation of biofilm on the surface. This open-cell foam provided a larger protected surface area for biofilm formation in the bioreactor. Moreover, the hydrophobic nature of PVDF open-cell foam facilitated the biofilm formation. On the other hand, in Figure 4.16 shows the SEM micrographs of the electrospun nanofibrous membranes after activated sludge filtration. The presence of biofilm was observed on the nanofibrous membranes with 0% MWCNT on some areas of the membranes. Comparatively less

amount of biofilm formation was observed on the surface of the membrane with MWCNT than the pristine PVDF membrane, due to the improved hydrophilicity of the surface of the membrane. Hydrophilic membranes are less likely to foul and hydrophobic membranes are more prone to foul because of the hydrophobic interaction between the membrane materials and microbial cells.

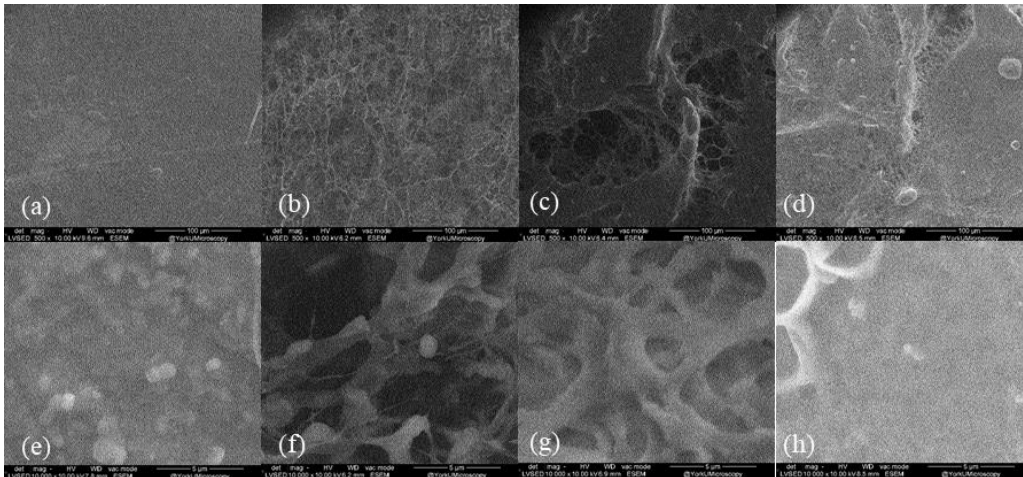


Figure 4.15: SEM micrographs of the feed side of the membranes at 500X with MWCNT loadings (a) 0 wt.%, (b)0.5 wt.% (c)1 wt.%, (d) 1.5wt.%; at 10kX with MWCNT loadings (e) 0 wt.%, (f) 0.5 wt.% (g)1 wt.%, (h) 1.5wt.%.

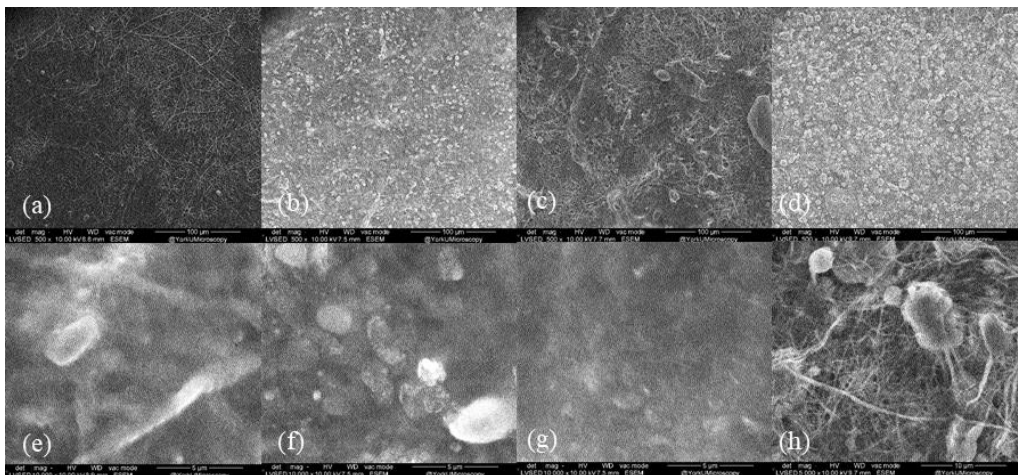


Figure 4.16: SEM micrographs of the permeate side of the membranes at 500X with MWCNT loadings (a) 0 wt.%, (b)0.5 wt.% (c)1 wt.%, (d) 1.5wt.%; at 10kX with MWCNT loadings (e) 0 wt.%, (f)0.5 wt.% (g)1 wt.%, (h) 1.5wt.%.

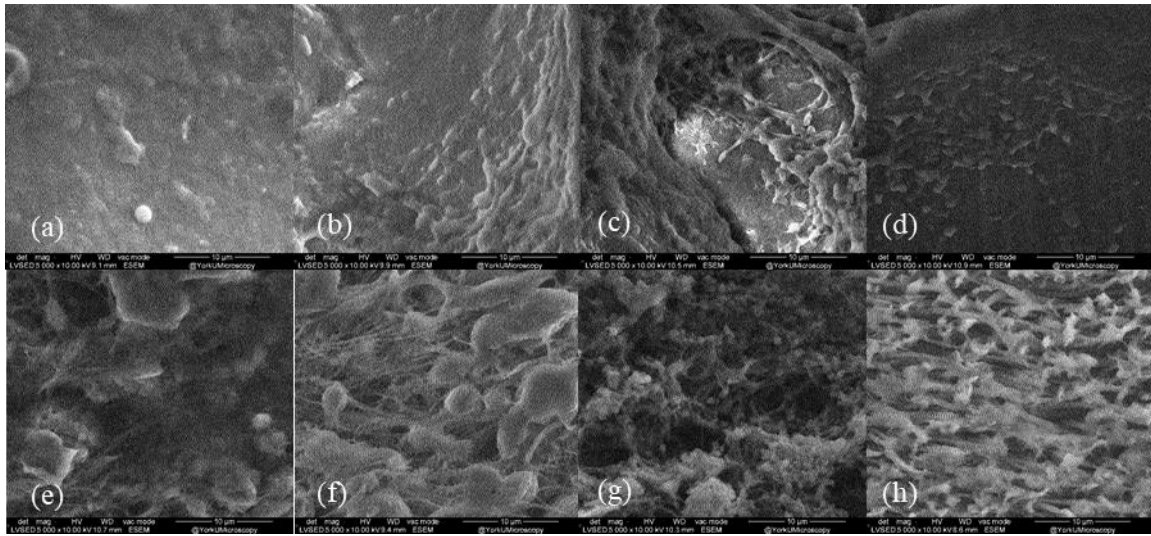


Figure 4.17: SEM micrographs of the cross-section of permeate side of the membranes at 5kX with MWCNT loadings (a) 0 wt.%, (b) 0.5 wt.% (c) 1 wt.%, (d) 1.5wt.%; cross-section of permeate side of the membranes with MWCNT loadings (e) 0 wt.%, (f) 0.5 wt.% (g) 1 wt.%, (h) 1.5wt.%.

Figure 4.17 (a-d) shows the SEM micrographs of the cross-section of the open-cell foam. The micrographs show the formation of biofilms inside the interconnected pores, which promoted the organic removal efficiency of the membranes. On the other hand, Figure 4.17 (e-h) shows the SEM micrographs of the cross-section of the nanofibrous membranes. The membrane with 0 wt.% MWCNT shows the presence of biofilm, but with an increasing amount of MWCNT contents, the presence of biofilm started to decrease. The membrane with 1.5 wt.% MWCNT shows almost no presence of biofilm in the cross-section

4.3. Conclusion

In this study, the effect of MWCNT loadings on the filtration performance and organic removal efficiency were studied. The water contact angles of the membranes showed that with increasing MWCNT loadings would improve the hydrophilicity of the membranes. The results obtained from pure water flux and synthetic wastewater flux showed that with an increasing amount of MWCNT

loading, the flux of the membrane increased. Improved hydrophilicity of the membranes after adding MWCNT increased the flux of the membranes. The activated sludge flux values of the membranes for two days experiment showed that 0.5% MWCNT membranes have higher flux than other membranes containing different amounts of MWCNT loading. This could be the variable thickness of the nanofibrous membranes. However, for 5 days and 10 days experiment the results showed that the flux increased with increasing amount of MWCNT loadings. And the fouling recovery ratio improved to 60% after the addition of MWCNT nanoparticles, which indicated the reusability of the membranes in the bioreactors.

SEM micrographs of the membranes on the seed side showed that the open-cell foams were fully covered by the biofilm on the surface and inside the pores of the foams. This indicated the microorganism's compatibility with PVDF open-cell foam as a biofilm carrier. However, the nanofibrous membranes with MWCNT loading were less likely to attach biofilm on the surface due to their hydrophilic nature.

Chapter Five: Conclusions and Recommendations

5.1. Conclusions

Membrane bioreactor is an efficient process for industrial and municipal wastewater treatment, which has provided noticeable advantages such as lower space requirement, low production of activated sludge and high grade of effluent. However, membrane fouling is restricting the use of membrane technology in membrane bioreactors by affecting the permeability of the membranes. This research aims to design and manufacture a multifunctional membrane system combining polymeric open-cell foam and nanoparticles embedded nanofibrous membranes to achieve different functionalities to improve the performance of the membrane bioreactors.

The first phase of this research revealed the effect of processing parameters of electrospinning process such as applied voltage, solution flow rate, and tip to collector distance on the morphology of the nanofibrous membranes. The SEM micrographs revealed that with increasing flow rate, the fiber diameter decreases and the formation of beads with a higher flow rate of 1.5 ml/h. The instability of the spinning jet with a high flow rate could be a reason for the formation of beads. The effect of applied voltage revealed that there is no significant change of pore size and porosity with the applied voltage. The experimental results showed that with the tip to collector distance the fiber diameter decreased due to the weakening the of the electric field strength after increasing the tip to collector distance. PVDF nanofibrous membranes with 0 wt.% MWCNT, 0.5 wt.% MWCNT, 1 wt.% MWCNT, and 1.5 wt.% MWCNT were prepared via electrospinning process with the combination of the processing parameters of 20 kV applied voltage, 15 cm tip to collector distance, and 1 mL/h flow rate as it gave the bead-less fibers with higher porosity. After incorporating MWCNT in the spinning solution, the fiber diameter

decreased which could be due to the increase in conductivity of the spinning solution. Moreover, it is believed that agglomeration of the MWCNT nanoparticles might contribute to this phenomenon. These nanoparticles embedded nanofibrous membrane were used in the second phase to prepare a multifunctional membrane with different layers.

In the second phase, multifunctional membranes were prepared by combining two different layers of PVDF open-cell foam and PDVF nanofibrous membrane with varying amount of MWCNT loadings (i.e., 0 wt.% MWCNT, 0.5wt.% MWCNT, 1wt.% MWCNT, and 1.5wt.% MWCNT). PVDF open-cell foams were prepared by fabrication approach that integrates compression molding and particulate leaching (e.g., 80 wt.% NaCl). The nanofibrous membrane was prepared via electrospinning by the same method as the first phase. Then, these two layers were attached together with the ScCO₂ foaming process. Herein, the open-cell foams were used as a biofilm carrier to improve the organic removal efficiency and the nanoparticles embedded nanofibrous membranes were used to provide the antifouling and antibacterial effect on the other side of the membrane. The proposed membrane systems were used in the membrane bioreactor to investigate the effect of different layers of the membranes and the MWCNT contents on the morphology, surface property, and filtration performance of the membranes.

The contact angles of the membranes with different MWCNT loadings showed that with an increasing amount of MWCNT loadings, the contact angle had been decreased. This indicates that the addition of MWCNT nanoparticles with PVDF spinning solution improved the hydrophilicity of the membranes. The pure water flux of the membranes with 1.5 wt.% MWCNT contents show 2 times higher flux than the membrane without MWCNT loadings. The flux with synthetic wastewater showed a similar trend of increase of flux after addition of MWCNT loadings but

compared to the pure water flux, the flux was lower because of the particulates present in the synthetic wastewater. The flux with activated sludge for 5 days and 10 days experiments showed that the membrane with 1.5 wt.% MWCNT contents have higher flux than the bare PVDF membranes. The fouling recovery ratio of membranes was reached 60% after addition of MWCNT nanoparticles, which indicated the reusability of the membranes in the membrane bioreactor in multiple cycles. Moreover, the membrane retention efficiencies of all the membranes after 5 days and 10 days filtration tests were above 90%, which indicates that the particulate removal was not affected by the membrane hydrophilicity.

The SEM micrographs showed that the presence of biofilm formation on the surface of the open-cell foam. The presence of biofilm on the cross-section of the open-cell foam confirms that the surfaces of all pores were fully covered by the biofilm. The hydrophobic nature of the PVDF foam and the higher surface area facilitated the biofilm formation by immobilizing the microorganisms. The SEM micrographs of the nanofibrous membranes showed that few areas were covered by biofilms, and with the increasing amount of MWCNT contents, there was less amount of biofilms. The electrospun membranes with MWCNT showed superior characteristics and antifouling properties in comparison with the pristine PVDF membranes in terms of hydrophilicity, pure water flux, synthetic wastewater flux and activated sludge flux.

This novel multifunctional membrane structure with MWCNT provided two different functionalities such as improved antifouling property of the membrane and higher organic removal efficiency to achieve a higher-grade effluent. The electrospun nanofibrous membrane with MWCNT improved the hydrophilicity and antifouling property of the membranes while the open cell foam maintained the higher organic removal efficiency. However, manufacturing electrospun

nanofibrous membrane and attaching the membrane with the open cell foam for industrial scale membrane module can be economically challenging.

5.2 Recommendation for future work

The aim of this research was to design and manufacture a multifunctional membranes platform to improve the antifouling property and the organic removal efficiency. To prepare the nanofibrous membrane electrospinning was adapted. With smaller pore size and higher porosity electrospinning has been studied in various fields for fabrication of fibers. However, the formation of beads was observed after incorporating the MWCNT nanoparticles in the PVDF polymer solution in the nanofibrous membrane structure. Better dispersion of MWCNT may reduce the agglomeration of the nanoparticles which as a result may give finer nanofibers without any beads. Further studies can be done to avoid the agglomeration the nanoparticles in the spinning solution to get the beadless fibers. In this study, addition of MWCNT with polymer solution improved the antifouling property of the membranes by improving the hydrophilicity of the membrane surface, further studies can be done with other nanomaterials to improve the hydrophilicity of the membrane. As hydrophilicity of membranes is an important factor for the permeation of the membranes, the other methods such as plasma treatment, surface modification by polymer grafting can be used to prepare superhydrophilic membranes. Superhydrophilic membranes will provide better antifouling property and will increase the permeation of the flux. The effect of different wastewater sources such as domestic and industrial wastewater on the performance multifunctional membranes can be investigated as these wastewaters contain different elements in terms of chemical compounds and organics. Moreover, for future experiments lab scale membrane bioreactor can be used to investigate the membrane performance to get precise experimental

results. Additionally, moving the developed multifunctional membranes platform into a prototype model to implement it into an industrial membrane and tested with pilot scale biosystem.

References

- [1] Shirazi, M., Kargari, A. and Shirazi, M. (2012). Direct contact membrane distillation for seawater desalination. *Desalination and Water Treatment*, 49(1-3), pp.368-375.
- [2] Sebastián Delgado, Enrique González, Miriam Morales and Rafael Villarroel (2011). *Aerobic Membrane Bioreactor for Wastewater Treatment - Performance Under Substrate-Limited Conditions*. INTECH Open Access Publisher.
- [3] Ghosh, A., Jeong, B., Huang, X. and Hoek, E., 2008. Impacts of reaction and curing conditions on polyamide composite reverse osmosis membrane properties. *Journal of Membrane Science*, 311(1-2), pp.34-45
- [3] Liao, Y., Loh, C., Tian, M., Wang, R. and Fane, A. (2018). Progress in electrospun polymeric nanofibrous membranes for water treatment: Fabrication, modification and applications. *Progress in Polymer Science*, 77, pp.69-94.
- [4] Lalia, B., Kochkodan, V., Hashaikeh, R. and Hilal, N. (2013). A review on membrane fabrication: Structure, properties and performance relationship. *Desalination*, 326, pp.77-95.
- [5] Jhaveri, J. and Murthy, Z. (2016). A comprehensive review on anti-fouling nanocomposite membranes for pressure driven membrane separation processes. *Desalination*, 379, pp.137-154.
- [6] Bawab, A., Ghannam, N., Abu-Mallouh, S., Bozeya, A., Abu-Zurayk, R., & Al-Ajlouni, Y. et al. (2018). Olive mill wastewater treatment in Jordan: A Review. *IOP Conference Series: Materials Science And Engineering*, 305, 012002. doi: 10.1088/1757-899x/305/1/012002

- [7] Mingchao, L., Tianzhi, W., Yunkai, L., Peiling, Y., Chengcheng, L., Pengxiang, L. and Wei, Z., 2013. Structural and fractal characteristics of biofilm attached on the surfaces of aquatic plants and gravels in the rivers and lakes reusing reclaimed wastewater. *Environmental Earth Sciences*, 70(5), pp.2319-2333.
- [8] Jianlong, W., Hanchang, S., & Yi, Q. (2000). Wastewater treatment in a hybrid biological reactor (HBR): effect of organic loading rates. *Process Biochemistry*, 36(4), 297-303. doi: 10.1016/s0032-9592(00)00153-9
- [9] Membrane bioreactors – multitube configurations. (2021). Retrieved 26 April 2021, from <https://www.thembrsite.com/mbr-multitube-configurations/>
- [8] Drioli, E. and Giorno, L., 2009. *Membrane Operations*. Weinheim: Wiley-VCH.
- [10] Pinnau, I. and Freeman, B., 2000. *Membrane Formation And Modification*. Washington, DC: American Chemical Society.
- [11] Baker, R. (2013). *Membrane technology and applications*. Hoboken, N.J.: Wiley.
- [12] Petersen, R., 1993. Composite reverse osmosis and nanofiltration membranes. *Journal of Membrane Science*, 83(1), pp.81-150.
- [13] Cadotte, J., Petersen, R., Larson, R. and Erickson, E., 1980. A new thin-film composite seawater reverse osmosis membrane. *Desalination*, 32, pp.25-31.
- [14] Prakash Rao, A., Desai, N. and Rangarajan, R., 1997. Interfacially synthesized thin film composite RO membranes for seawater desalination. *Journal of Membrane Science*, 124(2), pp.263-272.

- [15] Roh, I., Greenberg, A. and Khare, V., 2006. Synthesis and characterization of interfacially polymerized polyamide thin films. *Desalination*, 191(1-3), pp.279-290.
- [16] Ghosh, A., Jeong, B., Huang, X., & Hoek, E. (2008). Impacts of reaction and curing conditions on polyamide composite reverse osmosis membrane properties. *Journal Of Membrane Science*, 311(1-2), 34-45. doi: 10.1016/j.memsci.2007.11.038
- [17] Veríssimo, S., Peinemann, K. and Bordado, J., 2006. Influence of the diamine structure on the nanofiltration performance, surface morphology and surface charge of the composite polyamide membranes. *Journal of Membrane Science*, 279(1-2), pp.266-275.
- [18] Korikov, A., Kosaraju, P. and Sirkar, K., 2006. Interfacially polymerized hydrophilic microporous thin film composite membranes on porous polypropylene hollow fibers and flat films. *Journal of Membrane Science*, 279(1-2), pp.588-600.
- [19] Tarboush, B., Rana, D., Matsuura, T., Arafat, H., & Narbaitz, R. (2008). Preparation of thin-film-composite polyamide membranes for desalination using novel hydrophilic surface modifying macromolecules. *Journal Of Membrane Science*, 325(1), 166-175. doi: 10.1016/j.memsci.2008.07.037
- [20] Sarada, T., Sawyer, L. and Ostler, M., 1983. Three-dimensional structure of celgard® microporous membranes. *Journal of Membrane Science*, 15(1), pp.97-113.
- [21] Trommer, K. and Morgenstern, B., 2010. Nonrigid microporous PVC sheets: Preparation and properties. *Journal of Applied Polymer Science*, 115(4), pp.2119-2126.

- [22] Toimil-Molares, M., 2012. Characterization and properties of micro- and nanowires of controlled size, composition, and geometry fabricated by electrodeposition and ion-track technology. *Beilstein Journal of Nanotechnology*, 3, pp.860-883.
- [23] Komaki, Y. and Tsujimura, S., 1976. Growth of fine holes in polyethylenephthalate film irradiated by fission fragments. *Journal of Applied Physics*, 47(4), pp.1355-1358.
- [24] Shirikova, V. and Tretyakova, S., 1997. Physical and chemical basis for the manufacturing of fluoropolymer track membranes. *Radiation Measurements*, 28(1-6), pp.791-798.
- [24] J.H. Wendorff, S. Agarwal, A. Greiner, *Electrospinning: Materials, Processing, and Application*, Wiley, 2012.
- [25] Ahmed, F., Lalia, B. and Hashaikeh, R., 2015. A review on electrospinning for membrane fabrication: Challenges and applications. *Desalination*, 356, pp.15-30.
- [26] Antunes, M. and Velasco, J., 2014. Multifunctional polymer foams with carbon nanoparticles. *Progress in Polymer Science*, 39(3), pp.486-509.
- [27] Klempner, D., 1991. *Handbook Of Polymeric Foams And Foam Technology*. Munich: Hanser, pp.5-15.
- [28] Ghahramani, P., 2018. *Design And Fabrication Of Open-Cell Foams For Biological Organic Removal From Wastewater*. Master of Applied Science. York University.
- [29] Conoscenti, G., Carrubba, V. and Brucato, V., 2017. A Versatile Technique to Produce Porous Polymeric Scaffolds: The Thermally Induced Phase Separation (TIPS) Method. *Archives in Chemical Research*, 01(02).

- [30] Onder, O., Yilgor, E. and Yilgor, I., 2018. Preparation of monolithic polycaprolactone foams with controlled morphology. *Polymer*, 136, pp.166-178.
- [31] Whang, K., Thomas, C., Healy, K. and Nuber, G., 1995. A novel method to fabricate bioabsorbable scaffolds. *Polymer*, 36(4), pp.837-842.
- [32] Mosanenzadeh, S., Naguib, H., Park, C. and Atalla, N., 2013. Development of polylactide open-cell foams with bimodal structure for high-acoustic absorption. *Journal of Applied Polymer Science*, 131(7), p.n/a-n/a.
- [33] Zhang, C., Yuan, X., Wu, L., Han, Y. and Sheng, J., 2005. Study on morphology of electrospun poly (vinyl alcohol) mats. *European Polymer Journal*, 41(3), pp.423-432.
- [34] Yee, W., Kotaki, M., Liu, Y. and Lu, X., 2007. Morphology, polymorphism behavior and molecular orientation of electrospun poly(vinylidene fluoride) fibers. *Polymer*, 48(2), pp.512-521.
- [35] Bhardwaj, N. and Kundu, S., 2010. Electrospinning: A fascinating fiber fabrication technique. *Biotechnology Advances*, 28(3), pp.325-347.
- [36] Wannatong, L., Sirivat, A. and Supaphol, P., 2004. Effects of solvents on electrospun polymeric fibers: preliminary study on polystyrene. *Polymer International*, 53(11), pp.1851-1859.
- [37] Kulkarni, A., Bambole, V., & Mahanwar, P. (2010). Electrospinning of Polymers, Their Modeling and Applications. *Polymer-Plastics Technology And Engineering*, 49(5), 427-441. doi: 10.1080/03602550903414019
- 30 [38] Yuan XY, Zhang YY, Dong CH, Sheng J. Morphology of ultrafine polysulfone fibers prepared by electrospinning. *Polym Int* 2004; 53:1704–10

- [39] Kim KH, Jeong L, Park HN, Shin SY, Park WH, Lee SC, et al. Biological efficacy of silk fibroin nanofiber membranes for guided bone regeneration. *J Biotechnol* 2005a;120: 327–39.
- [40] Lee JS, Choi KH, Ghim HD, Kim SS, Chun DH, Kim HY, et al. Role of molecular weight of a tactic poly (vinyl alcohol) (PVA) in the structure and properties of PVA nanofabric prepared by electrospinning. *J Appl Polym Sci* 2004; 93:1638–46.
- [41] Geng X, Kwon OH, Jang J. Electrospinning of chitosan dissolved in concentrated acetic acid solution. *Biomaterials* 2005; 26:5427–32
- [42] Ki CS, Baek DH, Gang KD, Lee KH, Um IC, Park YH. Characterization of gelatin nanofiber prepared from gelatin-formic acid solution. *Polymer* 2005; 46:5094–102.
- [43] Buchko CJ, Chen LC, Shen Y, Martin DC. Processing and microstructural characterization of porous biocompatible protein polymer thin films. *Polymer* 1999;40: 7397–407
- [44] Pham QP, Sharma U, Mikos AG. Electrospun poly (ϵ -caprolactone) microfiber and multilayer nanofiber/microfiber scaffolds: characterization of scaffolds and measurement of cellular infiltration. *Biomacromolecules* 2006;7:2796–805
- [45] Meng, F., Chae, S., Drews, A., Kraume, M., Shin, H. and Yang, F. (2009). Recent advances in membrane bioreactors (MBRs): Membrane fouling and membrane material. *Water Research*, 43(6), pp.1489-1512.
- [46] Drews, A., 2010. Membrane fouling in membrane bioreactors—Characterisation, contradictions, cause and cures. *Journal of Membrane Science*, 363(1-2), pp.1-28.
- [47] Iorhemen, O., Hamza, R. and Tay, J. (2016). Membrane Bioreactor (MBR) Technology for Wastewater Treatment and Reclamation: Membrane Fouling. *Membranes*, 6(2), p.33.

- [48] Hwang, B., Lee, W., Yeon, K., Park, P., Lee, C., Chang, i., Drews, A. and Kraume, M., 2008. Correlating TMP Increases with Microbial Characteristics in the Bio-Cake on the Membrane Surface in a Membrane Bioreactor. *Environmental Science & Technology*, 42(11), pp.3963-3968.
- [49] Spettmann, D., Eppmann, S., Flemming, H. and Wingender, J., 2007. Simultaneous visualisation of biofouling, organic and inorganic particle fouling on separation membranes. *Water Science and Technology*, 55(8-9), pp.207-210.
- [50] Malaeb, L., Le-Clech, P., Vrouwenvelder, J., Ayoub, G. and Saikaly, P., 2013. Do biological-based strategies hold promise to biofouling control in MBRs?. *Water Research*, 47(15), pp.5447-5463.
- [51] Vanysacker, L., Declerck, P., Bilad, M. and Vankelecom, I., 2014. Biofouling on microfiltration membranes in MBRs: Role of membrane type and microbial community. *Journal of Membrane Science*, 453, pp.394-401.
- [52] Vanysacker, L., Denis, C., Declerck, P., Piasecka, A., & Vankelecom, I. F. J. (2013). Microbial Adhesion and Biofilm Formation on Microfiltration Membranes: A Detailed Characterization Using Model Organisms with Increasing Complexity. *BioMed Research International*, 2013, 1–12. doi: 10.1155/2013/470867
- [56] Estela, C. R. L., & Ramos, P. (2012). Biofilms: A Survival and Resistance Mechanism of Microorganisms. *Antibiotic Resistant Bacteria - A Continuous Challenge in the New Millennium*. doi: 10.5772/28504
- [57] Flemming, H.-C., & Wingender, J. (2010). The biofilm matrix. *Nature Reviews Microbiology*, 8(9), 623–633. doi: 10.1038/nrmicro2415

- [58] Li, H., Fane, A., Coster, H., & Vigneswaran, S. (2003). Observation of deposition and removal behaviour of submicron bacteria on the membrane surface during crossflow microfiltration. *Journal of Membrane Science*, 217(1-2), 29–41. doi: 10.1016/s0376-7388(03)00066-
- [59] Jin, Y.-L., Lee, W.-N., Lee, C.-H., Chang, I.-S., Huang, X., & Swaminathan, T. (2006). Effect of DO concentration on biofilm structure and membrane filterability in submerged membrane bioreactor. *Water Research*, 40(15), 2829–2836. doi: 10.1016/j.watres.2006.05.040
- [60] Yun, M.-A., Yeon, K.-M., Park, J.-S., Lee, C.-H., Chun, J., & Lim, D. J. (2006). Characterization of biofilm structure and its effect on membrane permeability in MBR for dye wastewater treatment. *Water Research*, 40(1), 45–52. doi: 10.1016/j.watres.2005.10.035
- [61] Zhang, J., Chua, H., Zhou, J., & Fane, A. (2006). Factors affecting the membrane performance in submerged membrane bioreactors. *Journal of Membrane Science*, 284(1-2), 54–66. doi: 10.1016/j.memsci.2006.06.022
- [62] Hwang, B.-K., Lee, W.-N., Park, P.-K., Lee, C.-H., & Chang, I.-S. (2007). Effect of membrane fouling reducer on cake structure and membrane permeability in membrane bioreactor. *Journal of Membrane Science*, 288(1-2), 149–156. doi: 10.1016/j.memsci.2006.11.032
- [63] Lee, W.-N., Chang, I.-S., Hwang, B.-K., Park, P.-K., Lee, C.-H., & Huang, X. (2007). Changes in biofilm architecture with addition of membrane fouling reducer in a membrane bioreactor. *Process Biochemistry*, 42(4), 655–661. doi: 10.1016/j.procbio.2006.12.003
- [61] Guo, W., Ngo, H.-H., & Li, J. (2012). A mini-review on membrane fouling. *Bioresource Technology*, 122, 27–34. doi: 10.1016/j.biortech.2012.04.089

- [62] Zhang, J., Loong, W. L. C., Chou, S., Tang, C., Wang, R., & Fane, A. G. (2012). Membrane biofouling and scaling in forward osmosis membrane bioreactor. *Journal of Membrane Science*, 403-404, 8–14. doi: 10.1016/j.memsci.2012.01.032
- [63] Flemming, H.-C., & Wingender, J. (2001). Relevance of microbial extracellular polymeric substances (EPSs) - Part I: Structural and ecological aspects. *Water Science and Technology*, 43(6), 1–8. doi: 10.2166/wst.2001.0326
- [64] Rosenberger, S., & Kraume, M. (2002). Filterability of activated sludge in membrane bioreactors. *Desalination*, 146(1-3), 373–379. doi: 10.1016/s0011-9164(02)00515-5
- [65] Metzger, U., Le-Clech, P., Stuetz, R. M., Frimmel, F. H., & Chen, V. (2007). Characterisation of polymeric fouling in membrane bioreactors and the effect of different filtration modes. *Journal of Membrane Science*, 301(1-2), 180–189. doi: 10.1016/j.memsci.2007.06.016
- [66] Wang, L., Liu, H., Zhang, W., Yu, T., Jin, Q., Fu, B., & Liu, H. (2018). Recovery of organic matters in wastewater by self-forming dynamic membrane bioreactor: Performance and membrane fouling. *Chemosphere*, 203, 123–131. doi: 10.1016/j.chemosphere.2018.03.171
- [67] Zhou, J., Yang, F.-L., Meng, F.-G., An, P., & Wang, D. (2007). Comparison of membrane fouling during short-term filtration of aerobic granular sludge and activated sludge. *Journal of Environmental Sciences*, 19(11), 1281–1286. doi: 10.1016/s1001-0742(07)60209-5
- [68] Kimura, K., Yamato, N., Yamamura, H., & Watanabe, Y. (2005). Membrane Fouling in Pilot-Scale Membrane Bioreactors (MBRs) Treating Municipal Wastewater. *Environmental Science & Technology*, 39(16), 6293–6299. doi: 10.1021/es0502425

- [69] Rosenberger, S., Laabs, C., Lesjean, B., Gnirss, R., Amy, G., Jekel, M., & Schrotter, J.-C. (2006). Impact of colloidal and soluble organic material on membrane performance in membrane bioreactors for municipal wastewater treatment. *Water Research*, 40(4), 710–720. doi: 10.1016/j.watres.2005.11.028
- [70] Sheikholeslami, R. (1999). Composite fouling - inorganic and biological: A review. *Environmental Progress*, 18(2), 113–122. doi: 10.1002/ep.670180216
- [71] You, H., Tseng, C., Peng, M., Chang, S., Chen, Y., & Peng, S. (2005). A novel application of an anaerobic membrane process in wastewater treatment. *Water Science and Technology*, 51(6-7), 45–50. doi: 10.2166/wst.2005.0620
- [72] Costa, A., Depinho, M., & Elimelech, M. (2006). Mechanisms of colloidal natural organic matter fouling in ultrafiltration. *Journal of Membrane Science*, 281(1-2), 716–725. doi: 10.1016/j.memsci.2006.04.044
- [73] Kim, I. S., & Jang, N. (2006). The effect of calcium on the membrane biofouling in the membrane bioreactor (MBR). *Water Research*, 40(14), 2756–2764. doi: 10.1016/j.watres.2006.03.036
- [74] Mutamim, N.S.A.; Noor, Z.Z.; Hassan, M.A.A.; Yuniarto, A.; Olsson, G. Membrane bioreactor: Applications and limitations in treating high strength industrial wastewater. *Chem. Eng. J.* 2013, 225, 109–1
- [75] Mutamim, N., Noor, Z., Hassan, M., Yuniarto, A. and Olsson, G. (2013). Membrane bioreactor: Applications and limitations in treating high strength industrial wastewater. *Chemical Engineering Journal*, 225, pp.109-119.

- [76] Zhang, G., Ji, S., Gao, X. and Liu, Z. (2008). Adsorptive fouling of extracellular polymeric substances with polymeric ultrafiltration membranes. *Journal of Membrane Science*, 309(1-2), pp.28-35.
- [77] Zheng, J., He, A., Li, J., & Han, C. (2007). Polymorphism Control of Poly(vinylidene fluoride) through Electrospinning. *Macromolecular Rapid Communications*, 28(22), 2159-2162. doi: 10.1002/marc.200700544
- [78] Huang, L., Manickam, S. and McCutcheon, J. (2013). Increasing strength of electrospun nanofiber membranes for water filtration using solvent vapor. *Journal of Membrane Science*, 436, pp.213-220.
- [79] Gee, S., Johnson, B. and Smith, A. (2018). Optimizing electrospinning parameters for piezoelectric PVDF nanofiber membranes. *Journal of Membrane Science*, 563, pp.804-812.
- [80] Rambabu, K. and Velu, S. (2016). Modified polyethersulfone ultrafiltration membrane for the treatment of tannery wastewater. *International Journal of Environmental Studies*, 73(5), pp.819-826.
- [81] Fang X, Li J, Li X, Pan S, Sun X, et al. (2017) Iron-tannin-framework complex modified PES ultrafiltration membranes with enhanced filtration performance and fouling resistance. *J Col Interface Sci* 505:642-652.
- [82] hao, S., Yan, W., Shi, M., Wang, Z., Wang, J. and Wang, S. (2015). Improving permeability and antifouling performance of polyethersulfone ultrafiltration membrane by incorporation of ZnO-DMF dispersion containing nano-ZnO and polyvinylpyrrolidone. *Journal of Membrane Science*, 478, pp.105-116.

- [83] Mahlangu, O., Nackaerts, R., Thwala, J., Mamba, B. and Verliefde, A. (2017). Hydrophilic fouling-resistant GO-ZnO/PES membranes for wastewater reclamation. *Journal of Membrane Science*, 524, pp.43-55.
- [84] Rahimi, Z., Zinatizadeh, A. and Zinadini, S. (2015). Preparation of high antibiofouling amino functionalized MWCNTs/PES nanocomposite ultrafiltration membrane for application in membrane bioreactor. *Journal of Industrial and Engineering Chemistry*, 29, pp.366-374.
- [85] Lee, J., Chae, H., Won, Y., Lee, K., Lee, C., Lee, H., Kim, I. and Lee, J. (2013). Graphene oxide nanoplatelets composite membrane with hydrophilic and antifouling properties for wastewater treatment. *Journal of Membrane Science*, 448, pp.223-230.
- [86] Arribas, P., García-Payo, M., Khayet, M. and Gil, L. (2019). Heat-treated optimized polysulfone electrospun nanofibrous membranes for high performance wastewater microfiltration. *Separation and Purification Technology*, 226, pp.323-336.
- [87] Huang, L., Manickam, S. and McCutcheon, J. (2013). Increasing strength of electrospun nanofiber membranes for water filtration using solvent vapor. *Journal of Membrane Science*, 436, pp.213-220.
- [88] Kobayashi, S. and Müllen, K. (2019). *Encyclopedia of Polymeric Nanomaterials*. Berlin, Heidelberg: Springer Berlin Heidelberg.
- [89] Moradi, G., Zinadini, S., Rajabi, L. and Dadari, S. (2018). Fabrication of high flux and antifouling mixed matrix fumarate-alumoxane/PAN membranes via electrospinning for application in membrane bioreactors. *Applied Surface Science*, 427, pp.830-842.

- [90] Kim, J. and Van der Bruggen, B. (2010). The use of nanoparticles in polymeric and ceramic membrane structures: Review of manufacturing procedures and performance improvement for water treatment. *Environmental Pollution*, 158(7), pp.2335-2349.
- [91] Derakhshan, A. and Rajabi, L. (2012). Review on applications of carboxylate–alumoxane nanostructures. *Powder Technology*, 226, pp.117-129.
- [92] Moradi, G., Zinadini, S., Dabirian, F. and Rajabi, L. (2019). Polycitrate-para-aminobenzoate alumoxane nanoparticles as a novel nanofiller for enhancement performance of electrospun PAN membranes. *Separation and Purification Technology*, 213, pp.224-234.
- [93] Derakhshan, A., Karimnezhad, H. and Rajabi, L. (2013). Synthesis and characterization of a dendrimeric polycitrate-alumoxane nano composite. *Materials Chemistry and Physics*, 141(2-3), pp.951-959.
- [96] Boor, S. L.; Victor, K.; Raed, H.; Nidal H. (2013) A review on membrane fabrication: Structure, properties and performance relationship, *Desalination*, 326, 77-95.
- [94] Nittami, T., Tokunaga, H., Satoh, A., Takeda, M., & Matsumoto, K. (2014). Influence of surface hydrophilicity on polytetrafluoroethylene flat sheet membrane fouling in a submerged membrane bioreactor using two activated sludges with different characteristics. *Journal of Membrane Science*, 463, 183–189. doi: 10.1016/j.memsci.2014.03.064
- [95] Guglielmi, G., & Andreottola, G. (2010). Selection and Design of Membrane Bioreactors in Environmental Bioengineering. *Environmental Biotechnology*, 439–516. doi: 10.1007/978-1-60327-140-0_10

- [96] Maximous, N., Nakhla, G., & Wan, W. (2009). Comparative assessment of hydrophobic and hydrophilic membrane fouling in wastewater applications. *Journal of Membrane Science*, 339(1-2), 93–99. doi: 10.1016/j.memsci.2009.04.034
- [97] Du, X., Shi, Y., Jegatheesan, V., & Haq, I. U. (2020). A Review on the Mechanism Impacts and Control Methods of Membrane Fouling in MBR System. *Membranes*, 10(2), 24. doi: 10.3390/membranes10020024
- [98] Lee, J., Chae, H.-R., Won, Y. J., Lee, K., Lee, C.-H., Lee, H. H., ... Lee, J.-M. (2013). Graphene oxide nanoplatelets composite membrane with hydrophilic and antifouling properties for wastewater treatment. *Journal of Membrane Science*, 448, 223–230. doi: 10.1016/j.memsci.2013.08.017
- [99] Zhu, X. and Elimelech, M., 1997. Colloidal Fouling of Reverse Osmosis Membranes: Measurements and Fouling Mechanisms. *Environmental Science & Technology*, 31(12), pp.3654-3662.
- [100] Guglielmi, G. and Andreottola, G., 2011. ChemInform Abstract: Selection and Design of Membrane Bioreactors in Environmental Bioengineering. *ChemInform*, 42(33), p.no-no.
- [101] Rana, D. and Matsuura, T., 2010. Surface Modifications for Antifouling Membranes. *Chemical Reviews*, 110(4), pp.2448-2471.
- [102] Hashino, M., Katagiri, T., Kubota, N., Ohmukai, Y., Maruyama, T. and Matsuyama, H., 2011. Effect of surface roughness of hollow fiber membranes with gear-shaped structure on membrane fouling by sodium alginate. *Journal of Membrane Science*, 366(1-2), pp.389-397.

- [103] Liao, Y., Wang, R., Tian, M., Qiu, C., & Fane, A. (2013). Fabrication of polyvinylidene fluoride (PVDF) nanofiber membranes by electro-spinning for direct contact membrane distillation. *Journal Of Membrane Science*, 425-426, 30-39. doi: 10.1016/j.memsci.2012.09.023
- [104] Hekmati, A., Rashidi, A., Ghazisaeidi, R. and Drean, J., 2013. Effect of needle length, electrospinning distance, and solution concentration on morphological properties of polyamide-6 electrospun nanowebs. *Textile Research Journal*, 83(14), pp.1452-1466.
- [105] Barakat, N., Kanjwal, M., Sheikh, F., & Kim, H. (2009). Spider-net within the N6, PVA and PU electrospun nanofiber mats using salt addition: Novel strategy in the electrospinning process. *Polymer*, 50(18), 4389-4396. doi: 10.1016/j.polymer.2009.07.005
- [106] Tijing, L., Woo, Y., Shim, W., He, T., Choi, J., Kim, S. and Shon, H., 2016. Superhydrophobic nanofiber membrane containing carbon nanotubes for high-performance direct contact membrane distillation. *Journal of Membrane Science*, 502, pp.158-170
- [107] Qureshi, N., Annous, B., Ezeji, T., Karcher, P., & Maddox, I. (2011). Biofilm reactors for Industrial Bioconversion processes. *Industrial Chemistry*, 202-241. doi:10.1201/b13132-13
- [108] Duarte, A., Mano, J., & Reis, R. (2009). Supercritical fluids in biomedical and tissue engineering applications: a review. *International Materials Reviews*, 54(4), 214-222. doi: 10.1179/174328009x411181
- [109] GOPAL, R., KAUR, S., MA, Z., CHAN, C., RAMAKRISHNA, S., & MATSUURA, T. (2006). Electrospun nanofibrous filtration membrane. *Journal Of Membrane Science*, 281(1-2), 581-586. doi: 10.1016/j.memsci.2006.04.026